

Degradation of Fatty Acid Export Protein1 by Rhomboid-Like Protease11 Contributes to Cold Tolerance in *Arabidopsis*

Annalisa John^a, Moritz Krämer^b, Martin Lehmann^b, Hans-Henning Kunz^b, Fayezeh Aarabi^c, Saleh Alseekh^c, Alisdair Fernie^c, Frederik Sommer^d, Michael Schröda^d, David Zimmer^e, Timo Mühlhaus^e, Helga Peisker^f, Katharina Gutbrod^f, Peter Dörmann^f, Jens Neunzig^g, Katrin Philippa^g and H. Ekkehard Neuhaus^{a*}

^a Plant Physiology, University of Kaiserslautern, Erwin-Schrödinger-Str., D-67653 Kaiserslautern, Germany

^b Plant Biochemistry, Faculty of Biology, Ludwig-Maximilians-Universität Munich, 82152 Planegg-Martinsried, Germany

^c Max Planck Institut for Molecular Plant Physiology, Wissenschaftspark Golm, D-14476 Potsdam, Germany

^d Molecular Biotechnology and Systems Biology, University of Kaiserslautern, Erwin-Schrödinger-Str., D-67653 Kaiserslautern, Germany

^e Computational Systems Biology, University of Kaiserslautern, Erwin-Schrödinger-Str., D-67653 Kaiserslautern, Germany

^f Institute for Molecular Physiology and Biotechnology of Plants, IMBIO, University of Bonn, Karlrobert-Kreiten-Str. 13, D-53115 Bonn, Germany

⁹ Plant Biology, Center for Human and Molecular Biology (ZHMB), Saarland University, D-66123 Saarbrücken, Germany

* Address correspondence to:

25 Ekkehard Neuhaus, University of Kaiserslautern, Plant Physiology, Gottlieb Daimler-Str.
26 47, D-67653 Kaiserslautern, Germany

27 Tel.: +49-631-2052372

28 Fax: +49-631-205-2600

29 E-mail: neuhaus@rhrk.uni-kl.de

30 **Short title:** RBL11 regulates FAX1 protein abundance in cold

31 **One sentence summary:** Degradation of the inner envelope protein Fatty Acid Export1
32 via Rhomboid Like Protease11 represents a critical process to achieve cold and frost
33 tolerance in *Arabidopsis*

34

35 The author responsible for distribution of materials integral to the findings presented in
36 this article in accordance with the policy described in the Instructions for Authors is:
37 Ekkehard Neuhaus (neuhaus@rhrk.uni-kl.de).

38

39 **Abstract**

40 Plants need to adapt to different stresses to optimize growth under unfavorable conditions.
41 The abundance of the chloroplast envelope located Fatty Acid Export Protein1 (FAX1)
42 decreases after the onset of low temperatures. However, it was unclear how FAX1
43 degradation occurs and whether altered FAX1 abundance contributes to cold tolerance in
44 plants. The rapid cold-induced increase in rhomboid-like protease11 (RBL11) transcript,
45 the physical interaction of RBL11 with FAX1, the specific FAX1 degradation after RBL11
46 expression, and the absence of cold-induced FAX1 degradation in *rb11* loss-of-function
47 mutants suggest that this enzyme is responsible for FAX1 degradation. Proteomic
48 analyses showed that *rb11* mutants have higher levels of FAX1 and other proteins
49 involved in membrane lipid homeostasis, suggesting that RBL11 is a key element in the
50 remodeling of membrane properties during cold. Consequently, in the cold, *rb11* mutants
51 show a shift in lipid biosynthesis towards the eukaryotic pathway, which coincides with
52 impaired cold tolerance. To demonstrate that cold sensitivity is due to increased FAX1
53 levels, FAX1 overexpressors were analyzed. *rb11* and FAX1 overexpressor mutants
54 show superimposable phenotypic defects upon exposure to cold temperatures. Our re-
55 sults show that the cold-induced degradation of FAX1 by RBL11 is critical for *Arabidopsis*
56 to survive cold and freezing periods.

57

58 **Introduction**

59 The vast majority of vascular plants are sessile. One of their most remarkable
60 characteristics is their ability to cope with a wide range of environmental conditions. When
61 light intensity, temperature, or water and nutrient availability leave certain ranges,
62 corresponding stress stimuli trigger systemic responses such as genetic, metabolic, and,
63 to some extent, morphological changes. These processes lead to a new metabolic
64 homeostasis that allows the plant to successfully cope with the environmental challenge
65 (Obata and Fernie, 2012; Koevoets et al., 2016; Choudhury et al., 2017; Pommerrenig et
66 al., 2018; Garcia-Molina et al., 2020; Wang et al., 2020).

67 Changes in growth temperature are usually more rapid than changes in water or nutrient
68 availability. Accordingly, plants must rapidly initiate appropriate acclimation programs.
69 These efficient molecular responses are essential because temperature affects the two
70 main processes of photosynthesis, i.e., the light-driven electron transport across the
71 thylakoid membrane and the subsequent enzyme-catalyzed Calvin-Benson cycle, in
72 different ways. Thus, photosynthesis is markedly responsive to temperature changes, as
73 demonstrated in several species representing a broad spectrum of CO₂-fixing organisms
74 (Lin et al., 2012; Mackey et al., 2013; Walker et al., 2013; Song et al., 2014).

75 It is well-known that the composition of membrane lipids in plant cells exhibits a dynamic
76 remodeling after onset of low temperatures (Moellering et al., 2010; Li et al., 2015; Barnes
77 et al., 2016; Barrero-Sicilia et al., 2017). These structural changes comprise a higher
78 degree of desaturation and altered abundancies of different phospho-, sulfo- or galacto-
79 lipid species, which ensure sufficient extent of membrane fluidity under unfavorable
80 environmental conditions (Smallwood and Bowles, 2002).

81 In plants, lipid biosynthesis represents a complex metabolic network in which initial
82 metabolic steps in the plastids (e.g., chloroplasts) are connected to subsequent processes
83 at the Endoplasmic Reticulum (ER) (Li-Beisson et al., 2010; Nakamura, 2017; Hözl and
84 Dörmann, 2019; Lavell and Benning, 2019). Generally, for the *de novo* synthesis of both
85 classes of lipids, namely storage lipids (triacyl-glycerols, TAG) or membrane lipids (in
86 chloroplasts mainly glyco-, phospho glycerolipids; and extraplastidic membranes,
87 phosphoglycerolipids, sphingolipids, and sterol lipids) it is necessary that fatty acid synthe-

88 sis in plastids provides acyl-chains for subsequent steps located in both, the plastid and
89 the ER (Rawsthorne, 2002; Li-Beisson et al., 2010). Accordingly, the subsequent lipid
90 biosynthesis takes either place via the plastid located “prokaryotic pathway” or via the ER
91 located “eukaryotic pathway” (Roughan and Slack, 1982).

92 While TAG is synthesized in the ER, the biosynthesis of membrane lipid occurs in both
93 organelles the ER and in plastids (Li-Beisson et al., 2013). During membrane lipid
94 synthesis, the usage of fatty acids in chloroplasts or alternatively in the ER leads to
95 different types of structural lipids. Generally, plastids represent the major site for
96 phosphatidyl-glycerol (PG) synthesis and the exclusive site for mono- and digalactosyl-
97 diacylglycerol (MGDG and DGDG) biosynthesis, as well as for sulfoquinovosyl-
98 diacylglycerol (SQDG) assembly. The ER and plastids are responsible for the provision of
99 diacyl-glycerol (DAG) backbones which serve as a precursor for all ER-borne
100 phospholipids, including phosphatidylcholine (PC) and phosphatidylethanolamine (PE)
101 (Hagio et al., 2002; Andersson and Dörmann, 2009; Li-Beisson et al., 2010; Lavell and
102 Benning, 2019). (Hagio et al., 2002; Andersson and Dörmann, 2009; Li-Beisson et al.,
103 2010; Lavell and Benning, 2019). DAG synthesis in chloroplasts is particularly pronounced
104 under cold conditions because the Sensitive to Freezing2 (SFR2) enzyme transfers
105 galactosyl groups from MGDG to other galactolipids, resulting in the formation of
106 oligogalactolipids (Moellering et al., 2010; Barnes et al., 2016). Besides the plastid-
107 produced DAG, the ER-derived DAG moieties also act - after import into plastids - as
108 precursors for plastid lipid biosynthesis (Li-Beisson et al., 2010).

109 Each membrane type is defined by a characteristic lipid composition. This composition is
110 dynamic in response to changing environmental conditions with individual lipid mixtures
111 giving rise to specific membrane properties (van Meer et al., 2008; Li-Beisson et al., 2010;
112 Moellering et al., 2010). For example, at low temperatures, lipid remodeling maintains
113 membrane fluidity to prevent ion leakage, to keep carrier and receptor proteins functional
114 or to integrate novel protective proteins (Steponkus et al., 1977; Barrero-Sicilia et al.,
115 2017). Accordingly, plant mutants exhibiting altered activities of (i) selected fatty acid
116 biosynthesis enzymes, of (ii) fatty acid desaturases, of (iii) lipid transfer proteins or of (iv)
117 lipases might exhibit modified cold tolerance and photosynthesis properties (Miquel et al.,
118 1993; Welti et al., 2002; Khodakovskaya et al., 2006; Guo et al., 2013; Gao et al., 2020;

119 Schwenkert et al., 2023). The latter studies emphasize the impact of a proper membrane
120 lipid remodeling after the onset of low temperatures. In fact, it has been shown for various
121 species that low environmental temperatures lead to an upregulation of the chloroplast
122 located lipid biosynthesis pathway (Li et al., 2015). Although several proteins involved in
123 this process have been identified, the precise regulation responsible for this metabolic
124 shift is still unknown.

125 In contrast to chloroplasts, which are the site of fatty acid *de novo* synthesis in the cell (Li-
126 Beisson et al., 2010), the lipid biosynthesis pathway localized in the ER depends on import
127 of fatty acids from plastids. The molecular nature of transport proteins mediating export of
128 newly synthesized fatty acids from plastids had remained unknown for a long time (Wang
129 and Benning, 2012). However, with the identification of the protein Fatty Acid Export
130 Protein1 (FAX1) a first candidate was identified (Li et al., 2015) and the ability of FAX1 to
131 promote shuttling of fatty acids across membranes has been shown in recombinant
132 baker's yeast cells (Li et al., 2015). Furthermore, the absence of FAX1, which resides in
133 the plastid inner envelope membrane, leads apart from male sterility (Li et al., 2015; Zhu
134 et al., 2020) to decreased levels of ER-derived eukaryotic lipids, while the relative content
135 of PG, synthesized via the prokaryotic pathway, was increased. In contrast, FAX1
136 overexpressor lines exhibit an increased level of lipids assembled via the eukaryotic
137 pathway, e.g., more TAG (Li et al., 2015).

138 The chloroplast serves as a cellular hub coordinating genetic and molecular responses
139 required to acclimate to altered environmental conditions (Schwenkert et al., 2022). Thus,
140 all signals and each metabolite emitted from- or received by the chloroplast must pass the
141 inner-envelope membrane. Therefore, the inner-envelope proteome undergoes profound
142 changes in response to the onset of stress conditions (Nishimura et al., 2016; Pottosin
143 and Shabala, 2016; Wagner et al., 2016). Strikingly, FAX1 belongs to a group of inner
144 envelope proteins which exhibit a proteolytic degradation after exposure to low
145 temperatures, while other inner envelope proteins increase in their abundance
146 (Trentmann et al., 2020). The mechanism responsible for the decrease of FAX1 in
147 response to cold temperatures is elusive. In addition, it is unknown whether this
148 phenomenon represents an important molecular process required for a maximal tolerance
149 against low temperatures and/or frost.

150 Chloroplasts contain more than 2000 different soluble- or membrane bound proteins
151 (Abdallah et al., 2000) and more than 20 different proteases ensure proteome homeo-
152 stasis within the organelle (Nishimura et al., 2016). So far, two major classes of proteases
153 have been identified to cleave intrinsic inner-envelope proteins, the metallo-dependent
154 AAA type FtsH proteases (with the isoforms FtsH 7, 9, 11 and 12) and the rhomboid-like
155 (RBL) proteases (with the isoforms RBL 10 and 11) (Knopf et al., 2012; Wagner et al.,
156 2016; Adam et al., 2019).

157 Thus, the function of FAX1 and the pronounced impact of lipid remodeling on plant
158 acclimation to cold raise two timely questions: First, what is the mechanism responsible
159 for the rapid decline of FAX1 upon onset of cold? Second, is the cold-induced
160 downregulation of FAX1 a pleotropic response or is it important for low temperature
161 tolerance? To answer both questions, we searched for an interaction of a selective
162 protease with FAX1. It turned out, that FAX1 and RBL11 can physically interact, and that
163 this protease is responsible for the cold-induced downregulation of FAX1. In addition, we
164 have shown that under cold conditions, *rb/11* mutants exhibit physiological and molecular
165 phenotypes similar to FAX1 overexpressors. Furthermore, we show that a lack of FAX1
166 degradation in response to cold impairs the ability of *Arabidopsis* plants to cope with low
167 temperature and freezing. These findings contribute to our understanding of how plants
168 tolerate adverse environmental conditions, one of the most impressive traits required to
169 ensure plant productivity.

170

171 **Results**

172 **Transcript abundance of the plastid protease *RBL11* responds to cold treatments**

173 It was previously shown that the protein Fatty Acid Export Protein1 belongs to a small
174 group of inner envelope proteins which are downregulated in their abundance upon onset
175 of cold temperatures (Trentmann et al., 2020). While FtsH12 is critical for chloroplast
176 development (Mielke et al., 2020), FtsH11 and RBL10 activity affect either, the
177 temperature response or the membrane lipid composition, respectively (Chen et al., 2006;
178 Wagner et al., 2011; Lavell et al., 2019). Thus, in addition to FtsH11 and RBL10, we
179 initially focused on RBL11 (the besides RBL10 only other rhomboid-like protease at the
180 inner envelope) which was shown to be active in fully developed mesophyll chloroplasts
181 (Knopf et al., 2012).

182 To gain first insight into possible molecular interactions between the proteases and FAX1
183 we analyzed the transcription level of corresponding genes after transfer to 4°C (Figure
184 1A), the standard temperature in our laboratory to study cold effects (Patzke et al., 2019;
185 Cvetkovic et al., 2021). Initially, transcript levels of all three envelope proteases
186 accumulated in response to the shift towards cold growth conditions. After one week at
187 4°C the most pronounced *RBL11* mRNA change was detected, which had about 14-fold
188 higher abundance when compared to the beginning of this treatment (Figure 1A). Both,
189 *RBL10* and *FTSH11* mRNA amounts peaked at 4- or 7 times higher levels respectively,
190 after 7 days of cold treatment versus the start of the cold period (Figure 1A). The highest
191 levels of all three mRNAs were present after 14 days in cold conditions and from then on,
192 these three transcript levels declined in their abundance (Figure 1A).

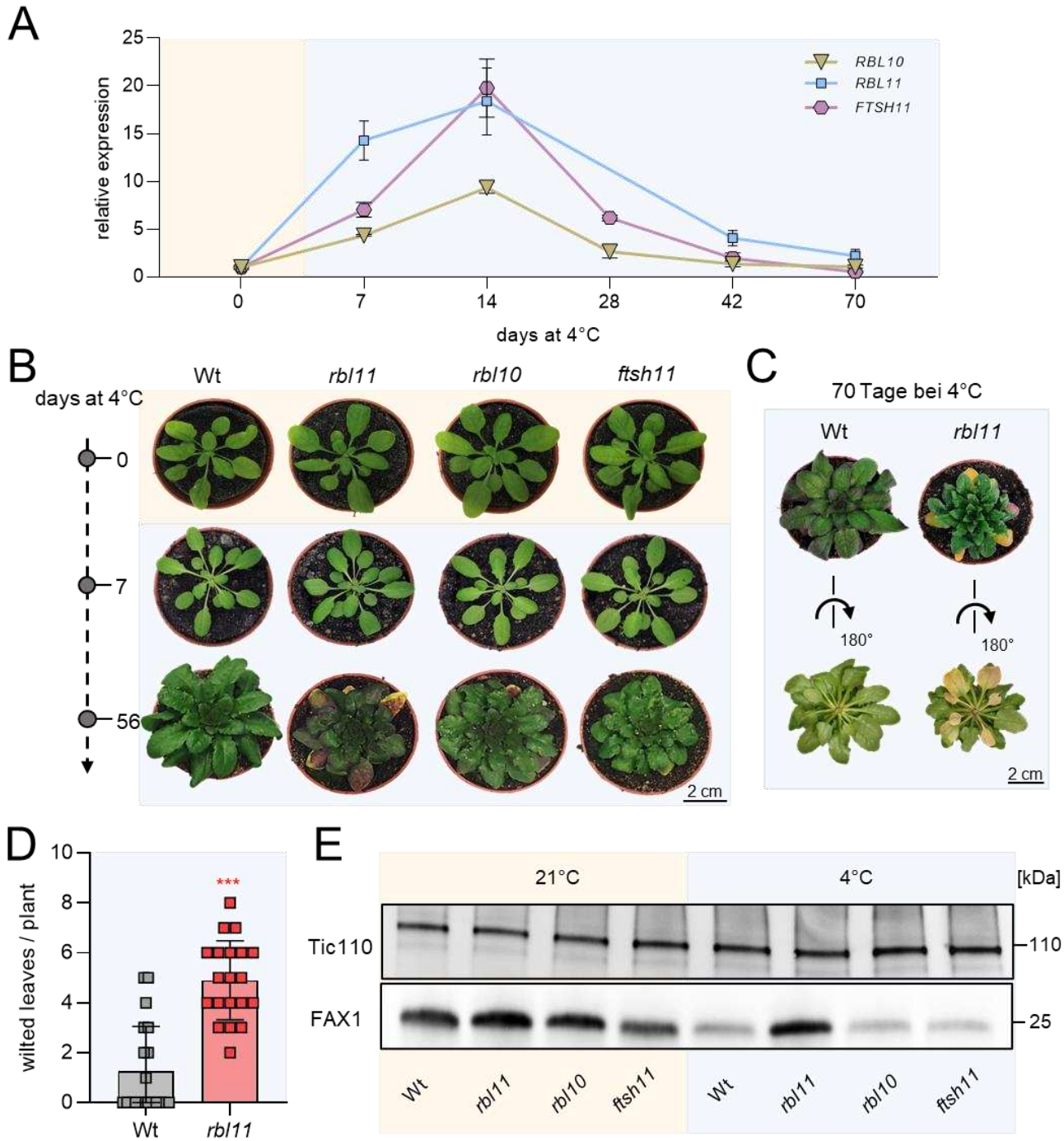
193

194 ***rbl11* mutants exhibit impaired growth at cold temperature since *RBL11* controls
195 FAX1 abundance in the cold**

196 To search for specific responses in mutants lacking one of the three proteases, we grew
197 wild-type and respective loss-of-function lines under either, control conditions (21°C), or
198 for 7 or 56 days at 4°C.

199 When grown at 21°C, none of the mutants exhibited a phenotypic pattern distinct from
200 wild-type plants (Figure 1B). When grown at 4°C for 7 days all genotypes showed slightly
201 decreased chlorophyll levels, as indicated by brighter leaves (Figure 1B). However, after
202 56 days at 4°C all mutant plants exhibited impaired growth, i.e., smaller rosette sizes when
203 compared to the wild type (Figure 1B). We previously showed that plants with impaired
204 tolerance against cold temperatures exhibited increased numbers of wilted leaves when
205 exposed to 4°C (Trentmann et al., 2020). Interestingly, after 56 days at 4°C, *rb/11* mutants
206 exhibited wilted leaves (Figure 1B). This effect was further exacerbated in *rb/11* plants
207 after ten weeks at 4°C (Figure 1C, pictures from top and bottom of the rosette). A
208 quantification of this observation showed that after ten weeks at 4°C, wild types exhibited
209 1.25 wilted leaves/plant, while *rb/11* mutants displayed in five wilted leaves per plant on
210 average (Figure 1D).

211 The observation that from all three proteases tested, the *RBL11* mRNA is the fastest
212 responding transcript within 7 days after transfer to 4°C (Figure 1A), rendered the
213 corresponding enzyme a prime candidate for cold-induced FAX1 degradation. To test the
214 effect of RBL11 on FAX1 levels, we isolated chloroplast envelopes from wild types and
215 *rb/11* loss-of-function mutant plants and conducted immunoblots using a previously
216 established FAX1 antibody (Li et al., 2015). The parallel immunoblotting of the inner
217 envelope protein TIC110 (Balsera et al., 2009) confirmed similar levels of total envelope
218 proteins in each lane (Figure 1E). Interestingly, already in *rb/11* mutants grown at control
219 temperature the FAX1 protein appeared increased by about 50% when compared to wild
220 type plants (Figure 1E). After 7 days in cold conditions, the FAX1 protein in wild type plants
221 decreased markedly (Figure 1E), which confirms our previous observations (Trentmann
222 et al., 2020). Such cold-induced FAX1 degradation was almost absent in *rb/11* mutants
223 compared to wild-type controls, while cold-induced FAX1 degradation occurred similarly
224 in *rb/10* and *ftsh11* mutants (Figure 1E).



225

226 **Figure 1:** Gene expression, phenotypic and immunoblot analysis of *Arabidopsis* protease loss-of-
227 function mutants *rbl11*, *rbl10* and *ftsh11* grown under standard and cold (4°C) conditions. Plants
228 were grown under standard conditions (21°C day and night temperature, 10h day length and
229 120μE light intensity) for 3 weeks and then treated with cold (4°C day and night temperature, 10h
230 day length and 120μE light intensity). A) Gene expression levels of *RBL11*, *FTSH11* and *RBL10*
231 in wild type by qRT-PCR under standard growth conditions (0 days at 4°C) and several days
232 during cold treatment (7; 14; 28; 42, and 70 days at 4°C). Data represent relative mean expression
233 levels of 3 biological replicates and are normalised to standard conditions (0 days at 4°C) using

234 UBQ as an internal control. B) Phenotypic analysis of *rbf11*, *rbf10* and *ftsh11* *Arabidopsis* plants.
235 Images were taken from plants grown under standard conditions and after chilling for 7 and 56
236 days. C) Wt and *rbf11* rosettes were cut after 70 days of cold treatment and rotated to highlight
237 the wilted leaves. D) Number of wilted leaves per plant in Wt and *rbf11* after 70 days of cold
238 treatment. E) Immunoblot analysis via FAX1 antibody in isolated chloroplast envelopes of Wt,
239 *rbf11*, *rbf10* and *ftsh11* from plants grown under standard conditions (21°C) and plants grown for
240 7 days at 4°C. Immunoblot detection via Tic110 antibody is used as a control and shows an equal
241 loading of the protein samples at 3 µg per lane. Error bars in A) represent ± SEM. Error bars in D)
242 are ± SD. Asterisks indicate significant differences between Wt and mutant using a t-test: p-value
243 ≤0.001: *** (Supplemental file 1).

244

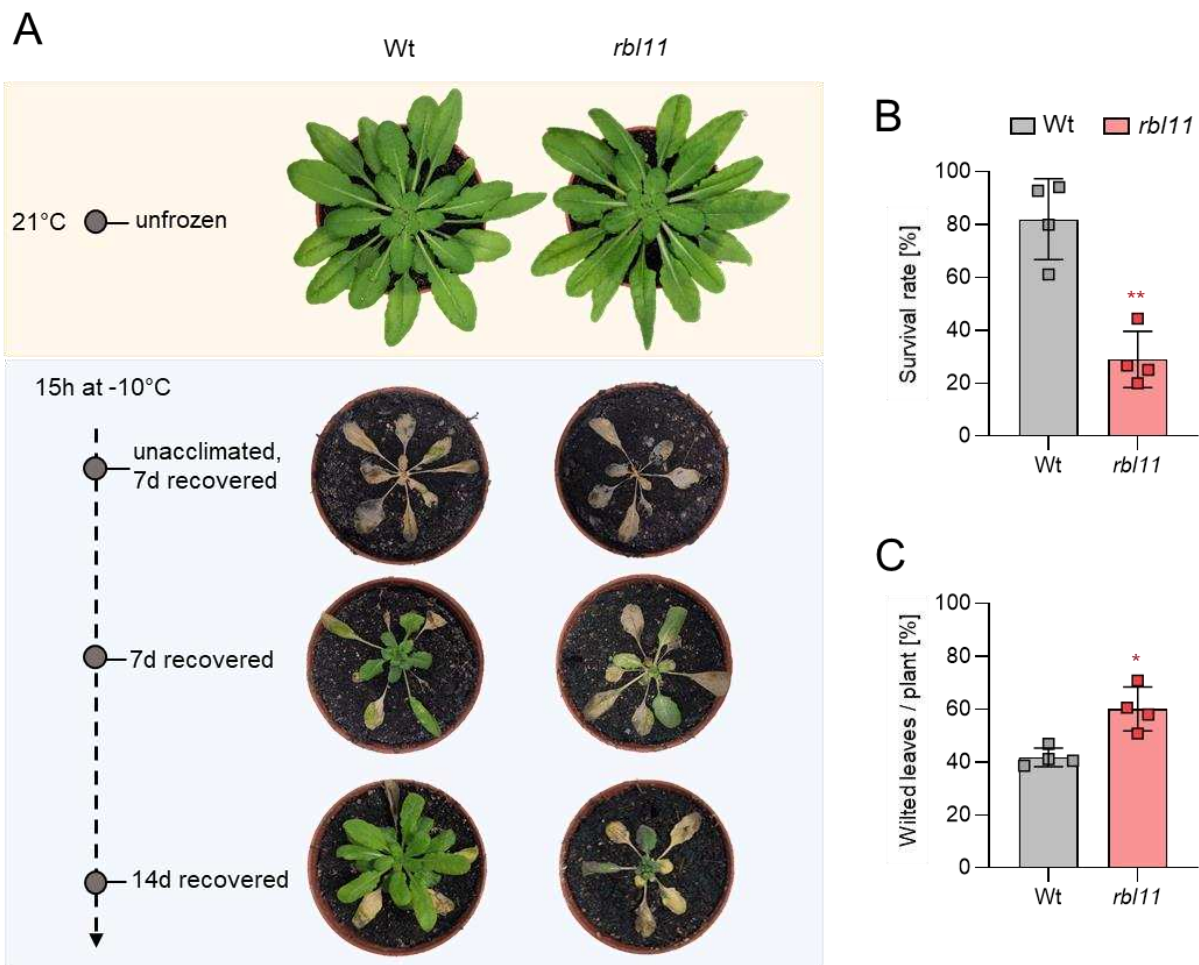
245 ***rbf11* mutants exhibit impaired frost tolerance**

246 The observation that *rbf11* plants show an increased number of wilted leaves when grown
247 at cold temperatures (Figure 1B-D) led us to test the freezing tolerance of this mutant. The
248 ability of vascular plants to withstand freezing temperatures depends on a pretreatment
249 of several days at temperatures above 0°C, called cold acclimation (Alberdi and Corcuera,
250 1991). To investigate whether the altered cold response in mutants affects freezing
251 tolerance, we compared the ability of wild-types and *rbf11* plants to recover from exposure
252 to freezing temperatures. To this end, plants were grown at 21°C and shifted to 4°C for
253 four days to acclimate the cold. The temperature was then gradually reduced (2°C/h) until
254 -10°C was reached. This temperature was maintained for 15h and then gradually
255 increased (2°C/h) to 21°C before re-lighting (Trentmann et al., 2020). We assessed the
256 phenotypic appearance of frost-treated plants after one and two additional weeks of
257 growth at 21°C and quantified the number of wilted leaves as well as the survival rate after
258 two weeks recovery phase.

259 As expected, unacclimated wild types and *rbf11* plants are unable to survive a freezing
260 treatment (Figure 2A). As seen previously (Trentmann et al., 2020), wild-type plants are
261 able to recover from a period of freezing with an efficiency of about 80% (Figure 2A,B)
262 and exhibited 42% wilted leaves (Figure 2C). In contrast, *rbf11* mutants showed a
263 significantly reduced ability to recover from freezing treatment, as only 28% of all plants
264 survived the freezing period and more than 60% of the leaves were wilted (Figure 2A-C).

265

266



267

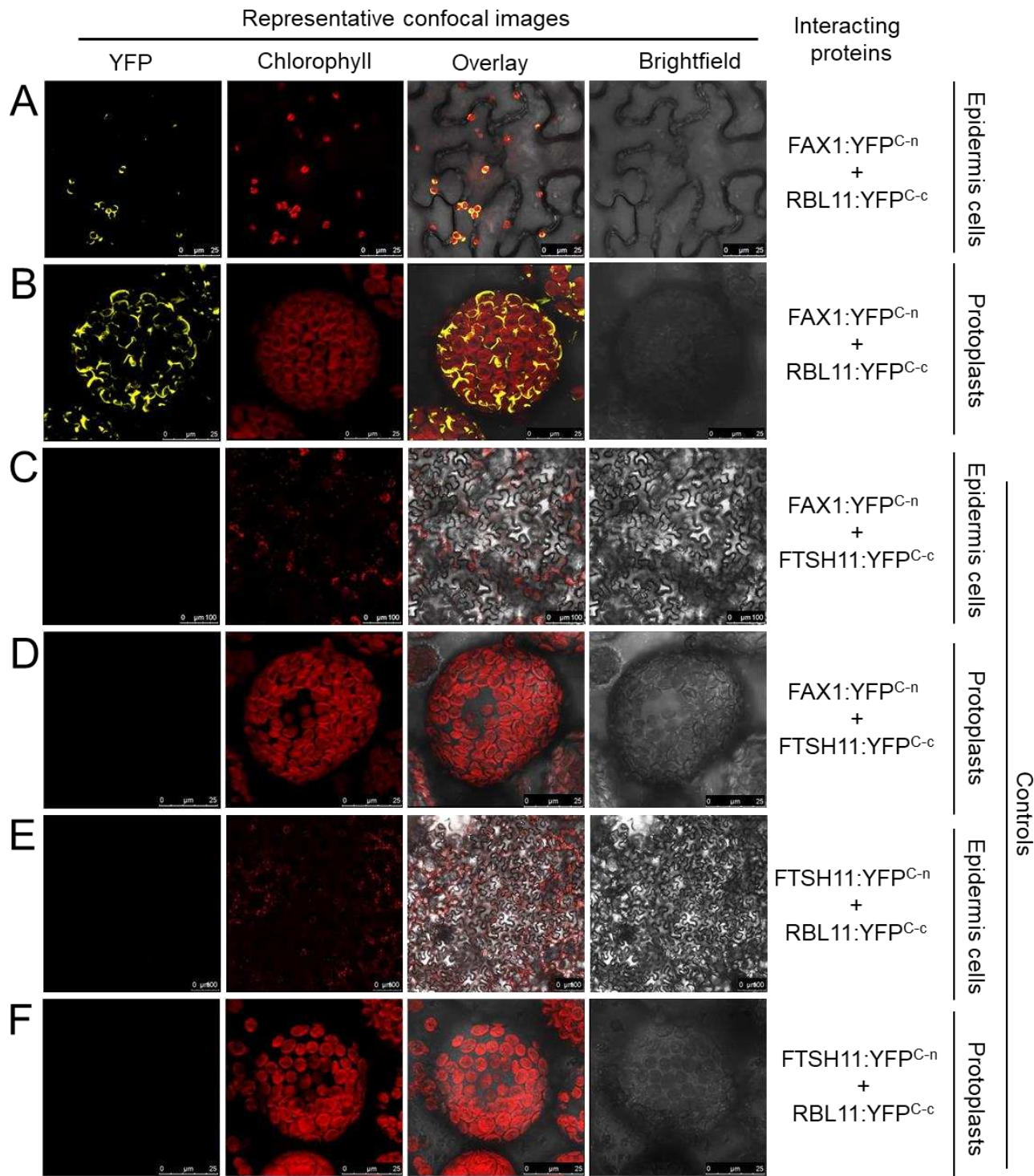
268 **Figure 2:** Recovery from freezing is impaired in *rbl11* loss-of-function mutants. Plants were grown
269 under standard growth conditions for 3 weeks. Prior to freezing, the temperature was lowered to
270 4°C for 4 days (day and night temperature) for cold acclimation. The lowering of the temperature
271 for freezing was done stepwise (2°C/h) and in complete darkness. The temperature for freezing
272 was maintained at -10°C for 15 h before being gradually increased to 21°C (2°C/h). A)
273 Representative Wt and *rbl11* plants recovered from -10°C freezing. Images were taken 7 and 14
274 days after freezing, from unacclimated and unfrozen (control) plants. B) Comparison of survival
275 between Wt and *rbl11* mutants 7 days after -10°C treatment. Data represent the mean of four
276 independent experiments with 10 to 20 plants per line and experiment. C) Quantification of wilted
277 leaves from Wt and *rbl11* plants recovered from -10°C freezing for 7 days under standard growth
278 conditions. Data are the mean of 4 independent experiments. Statistical differences between wild-
279 type and overexpressor lines in B) and C) were analysed by Student's t-test followed by Welch's
280 correction: p-value ≤0.05: *; p-value ≤0.01: ** (Supplemental file 1).

281

282 **RBL11 and FAX1 interact physically at the inner envelope membrane of chloro-**
283 **plasts**

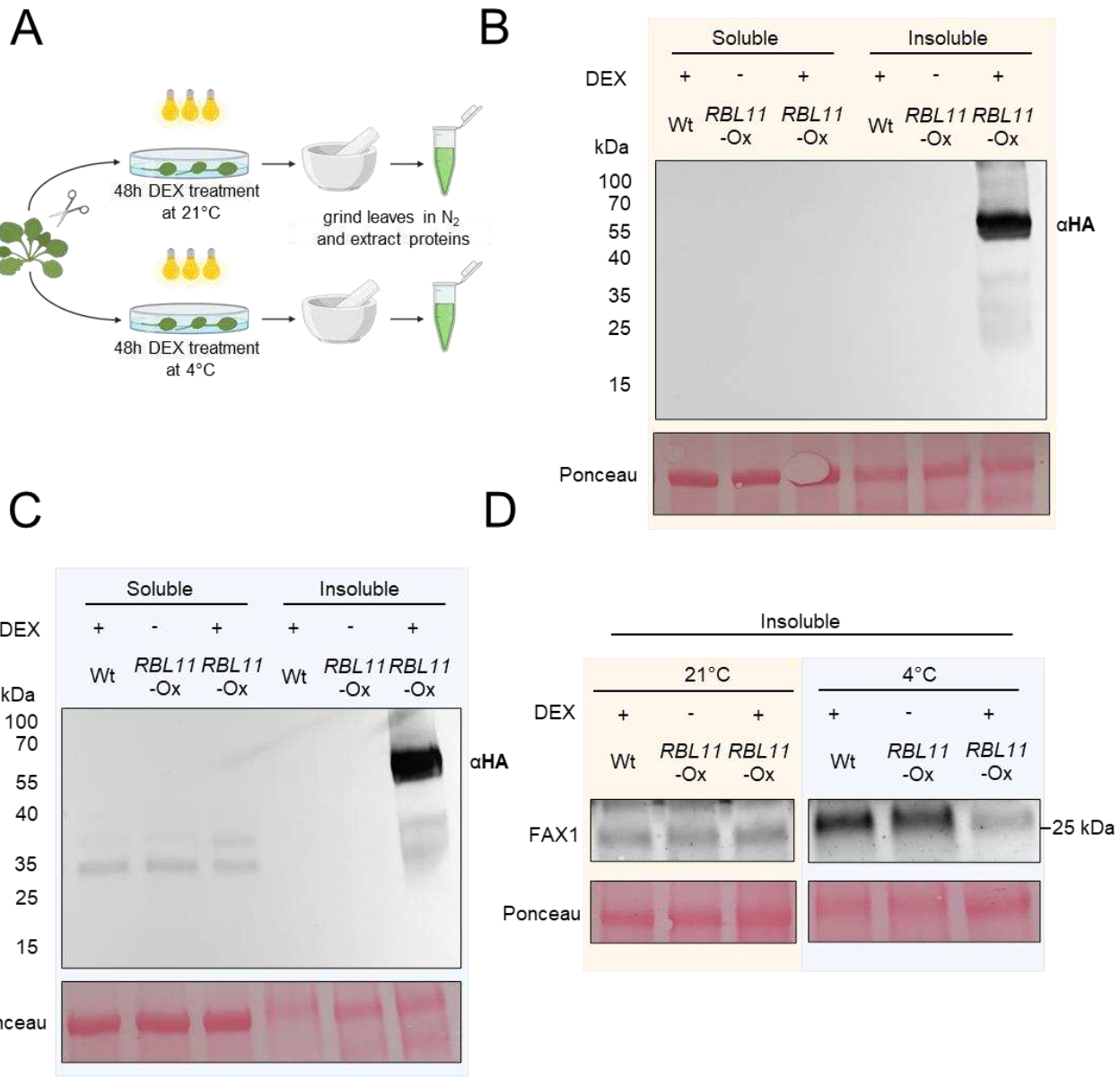
284 Having established that RBL11 activity is mandatory for cold-induced FAX1 degradation
285 (Figure 1E), we were next interested to probe for a direct physical interaction between
286 these two proteins. To this end, we exploited the Bimolecular Fluorescence
287 Complementation (BiFC) analysis (Kerppola, 2008) based on the association of
288 complementary yellow fluorescent protein (YFP) fragments fused to putative partner
289 proteins. Only when both partners are in close proximity, a functional fluorescent protein
290 can be formed, indicating the protein-protein interaction and its subcellular location within
291 the living cell.

292 We infiltrated *Nicotiana benthamiana* leaves with the constructs FAX1:YFP^{C-n} and
293 RBL11:YFP^{C-c} for synthesis of the respective YFP fragment proteins. Co-expression of both
294 constructs resulted in yellow fluorescing spots in epidermis cells (Figure 3A), indicating
295 that both proteins interact in corresponding plastids. To further visualize the complex
296 formation of both proteins at the chloroplast envelope, we infiltrated *N. benthamiana*
297 leaves with both constructs and subsequently isolated mesophyll protoplasts. The
298 combined expression of FAX1:YFP^{C-n} and RBL11:YFP^{C-c} led to a yellow fluorescence of
299 chloroplasts (Figure 3B). The ring-shaped fluorescence (Figure 3B) resembles the YFP
300 fluorescence emitted by other inner envelope associated YFP fusion proteins (Witz et al.,
301 2014; Patzke et al., 2019). To validate the BiFC data we performed further control
302 experiments using inner envelope associated protease FtsH11. In contrast to the co-
303 expression of FAX1:YFP^{C-n} and RBL11:YFP^{C-c}, the infiltration of the plasmids with
304 FAX1:YFP^{C-n} and FTSH11:YFP^{C-c} did not yield fluorescence complementation (Figure
305 3C,D). In addition, the combined infiltration of the constructs FTSH11:YFP^{C-n} and
306 RBL11:YFP^{C-c} also did not give rise to a fluorescence signal (Figure 3E,F). These two
307 independent control experiments indicate that protein-protein interaction at the inner
308 envelope does not occur by chance, highlighting the specificity of the RBL11 and FAX1
309 interaction (Figure 3A,B).



317 **Induction of *RBL11* leads to a specific degradation of FAX1**

318 In contrast to wild types, *rb11* plants are almost unable to degrade FAX1 after the onset
319 of cold (Figure 1E). To further support our hypothesis that RBL11 is responsible for cold-
320 induced FAX1 degradation, we generated a stable RBL11-HA (HA = hemagglutinin) over-
321 expressor line in which the recombinant *rb11* gene was placed under the control of a
322 dexamethasone (DEX)-inducible promoter (Aoyama and Chua, 1997) (Figure 4A). In the
323 presence of DEX, the RBL11-HA protein is synthesized in mutant leaf discs at 21°C and
324 at 4°C (Figure 4B,C), and neither DEX-induced overexpression nor the C-terminal HA tag
325 alters the membrane localization of RBL11 (Figure 4B,C). Subsequent enrichment of total
326 leaf membranes, followed by immunoblot analysis using the FAX1-specific antibody,
327 showed that RBL11 overexpression does not lead to FAX1 degradation from leaf discs
328 incubated with DEX at 22°C (Figure 4D), which might be due to some post-translational
329 modification required for FAX1 activity. In contrast, DEX incubation at 4°C leads to FAX1
330 degradation (Figure 4D, note that extraction of total membrane proteins from whole
331 membranes enriched from cold treated leaf discs generally resulted in a higher abundance
332 of FAX1 (Figure 4D, left and right panels).

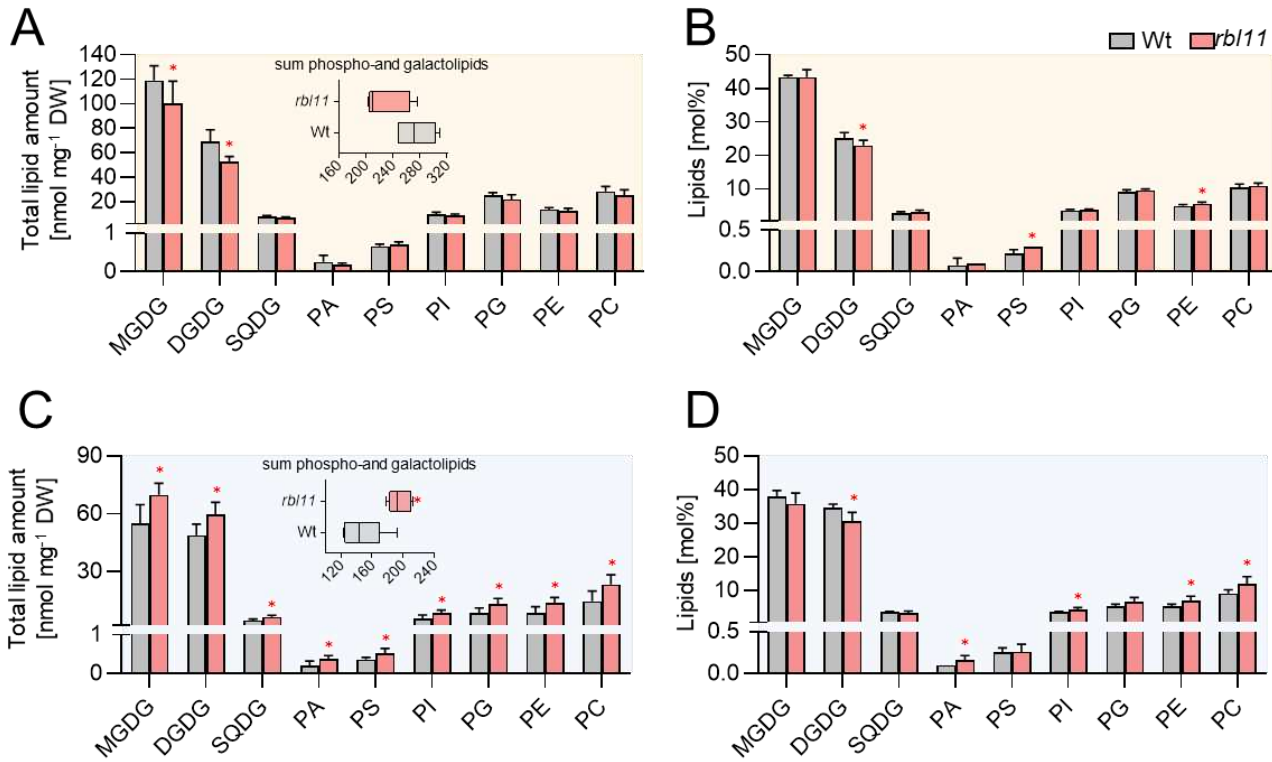


334 **Figure 4: Cold induced degradation of FAX1 by RBL11 in *Arabidopsis*.** A) Scheme of
335 experimental setup. B) Immunoblot analysis via HA antibody of soluble and insoluble (membrane)
336 protein extracts from wildtype and transgenic plants expressing *RBL11* tagged with a HA epitope
337 (~ 32 kDa) under the control of an 35S promoter after induction with dexamethasone for 48h at
338 21°C. C) Immunoblot detection via HA antibody of soluble and insoluble (membrane) protein
339 extracts from wildtype and transgenic plants expressing *RBL11* tagged with a HA epitope (~ 67
340 kDa) under the control of an 35S promoter after induction with dexamethasone for 48h at 4°C.
341 Note that the size of the protein (~ 67 kDa) comes from the presence of an additional biotinylase
342 (~35 kDa), which was not relevant in this experiment. D) Immunoblot of insoluble protein extracts
343 from Wt and transgenic plants overexpressing *RBL11* under the control of an 35S promoter
344 after induction with DEX for 48h at 21°C or 4°C with a FAX1 antibody. Please note that the
345 extraction of whole membranes enriched from cold treated leaves generally resulted in a higher
346 abundance of FAX1 and is not comparable with results from leaves treated at 21°C. Ponceau
347 staining in B), C) and D) is representing equal loading of protein samples with 18 µg per lane.

348 **The membrane lipid composition of *rb/11* mutants indicates a shift to the eukaryotic
349 biosynthesis pathway under low temperature**

350 The abundance of FAX1 strongly decreases after transfer of wild type to cold conditions
351 (Figure 1E and Trentmann et al. 2020). Because the absence of RBL11 prevents cold-
352 induced FAX1 degradation (Figure 1E) we aimed to determine changes in lipid levels
353 under these growth conditions. For this purpose, wild-type and *rb/11* mutant plants were
354 first grown for 4 weeks under control conditions and then either, for further 14 days at
355 21°C or at 4°C, prior to extraction and quantification of leaf lipids.

356 Growth of plants at 21°C led to lower leaf levels of the major glycolipids monogalactosyl-
357 diacylglycerol (MGDG) and digalactosyl-diacylglycerol (DGDG) in *rb/11* plants compared
358 to wild types (Figure 5). In contrast, the levels of sulfoquinovosyl-diacylglycerol (SQDG)
359 and the phospholipids phosphatidic acid (PA), phosphatidylserine (PS), phosphati-
360 dylinositol (PI), phosphatidylglycerol (PG), phosphatidylethanolamine (PE) and phospha-
361 tidylcholine (PC) were similar in leaves from the two plant lines (Figure 5). These absolute
362 amounts summed up to 230 nmol mg⁻¹ DW of phospho- and glycolipids in *rb/11* mutants
363 and 274 nmol mg⁻¹ DW of phospho- and glycolipids in wild-type plants (Figure 5A, inset).
364 However, after recalculating the data from total levels into mol% no obvious changes in
365 the relative individual lipid species between *rb/11* mutant and wild type plants were found
366 (Figure 5B). Interestingly, growth for 14 days under cold temperature conditions led to
367 higher total lipid levels in the *rb/11* plants (Figure 5C inset). This increase of total lipids in
368 the *rb/11* mutants is due to higher levels of MGDG, DGDG and SQDG, but also to higher
369 levels of all phospholipids (Figure 5C). Furthermore, after recalculating the data into mol%
370 it appeared that growth at 4°C did not only lead to higher total lipid contents in *rb/11* plants,
371 but that especially the relative proportions (in mol%) of the phospholipid species PA, PI,
372 PE and PC to the total lipids was increased in the *rb/11* plants, while proportions of MGDG
373 and DGDG are decreased (Figure 5D).



374

375 **Figure 5.** Analysis of galacto- and phospholipids in Wt and *rb11* loss-of-function mutants.
376 Changes in A) total contents and B) relative amounts of different galacto- and phospholipids in
377 rosette leaves of 3-week-old *Arabidopsis* plants grown under standard conditions. The box plot in
378 A) shows changes in the sum of the measured total lipid contents. Differences in C) total lipid
379 contents and D) relative galacto- and phospholipid amounts in plants grown under standard
380 conditions for 3 weeks before lowering the temperature to 4°C for 14 days. The box plot in C)
381 shows the changes in the sum of the measured total lipid contents. Data represent the mean of 5
382 plants per row. Error bars indicate \pm SD. Significance of differences between wild-type and mutant
383 was analysed by Student's t-test: p-value \leq 0.05: * (Supplemental file 1).
384

385 Identification of other putative RBL11 protease substrates

386 By analyzing the envelope proteome of *rb110rb11* double mutants an overrepresentation
387 of non-degraded envelope proteins compared to wild type emerged (Knopf et al., 2012).
388 However, this type of analysis did not allow for the identification of RBL11-specific
389 substrates. Thus, we compared the envelope proteome from wild type plants with that of
390 *rb11* single mutants (Table 1, Suppl. Table 1, Suppl. Table 2, and Suppl. Table 3). Since
391 we were especially interested in RBL11 substrates degraded after onset of cold tempe-
392 ratures, these analyses were carried out on plants grown at 21°C or at 4°C (Table 1).

393

Protein	Gene locus	Description	Log2FC	qValue_Interaction
			<i>rb11</i> / Wt	Genotype Temperature
TGD5	At1g27695	Encodes a small glycine rich protein that is localized to the chloroplast envelope and is a component of the ER to plastid lipid trafficking pathway.	4.54	0.033
PORA	At5g54190	light-dependent NADPH:protochlorophyllide oxidoreductase A	4.08	0.030
HCF107	At3g17040	Involved in regulating plastidial gene expression and biogenesis	1.56	0.002
unknown	At3g28220	TRAF-like family protein, contains MATH domain	2.73	0.044
KIN14A	At5g10470	Kinesin-like protein required for chloroplast movements and anchor to the plasma membrane	2.18	0.032
DVR	At5g18660	Encodes a protein with 3,8-divinyl protochlorophyllide a 8-vinyl reductase activity	1.85	0.031
unknown	At1g08530	Chitinase-like protein	1.35	0.019
unknown	At5g19850	Alpha/beta-Hydrolases superfamily protein	1.47	0.027
unknown	At1g64850	Calcium-binding EF hand family protein	1.22	0.015
unknown	At5g39410	Saccharopine dehydrogenase	1.06	0.018
unknown	At2g43630	Nucleus envelope protein	0.48	0.004
TGD2	At3g20320	Encodes a permease-like component of an ABC transporter involved in lipid transfer from ER to chloroplast. A phosphatidic acid-binding protein.	0.98	0.022
DEGP2	At2g47940	Encodes DegP2 protease	0.83	0.015
SPPA	At1g73990	Encodes a light-inducible chloroplast protease complex	0.78	0.015
FAX1*	At3g57280	involved in fatty acid and lipid homeostasis and likely functions as a fatty acid transporter that exports fatty acids from the plastid	0.38	0.028

394 Table 1. The table shows the 15 top hits of proteins that are increased by more than 30% in the mutant at low
 395 temperature. For each protein a two-way ANOVA was performed, which means that only proteins with a significance
 396 level below 0.05 were considered. The qValue_Interaction Genotype Temperature indicates that there is a temperature
 397 effect that differs between mutant and wild type. All proteins were annotated by name, gene locus and description. The
 398 proteins written in bold and in italics are increased under standard conditions as well as after 7 days at 4°C (see Suppl.
 399 Table 1) to the described selected criteria (Abundance > 30%; qValue < 0.05). FAX1 was labeled with an asterisk
 400 because the protein is not within the top hits, but also fulfills the selected criteria.

401 Putative substrates of RBL11 are expected to be more abundant in *rb11* mutants when
402 compared to wild-type plants. In a previous study on proteins accumulating in the inner
403 envelope of *rb10rb11* double mutants, the TRAF-like family protein containing a MATH
404 domain was also found to accumulate in the double mutant (Knopf et al., 2012). Similarly,
405 the TRAF-like family protein accumulated in *rb11* single mutants (Suppl. Table 1)
406 indicating that this protease is responsible for its degradation. Interestingly, the
407 abundance of the protein TGD5, which is involved in ER to plastid lipid transfer (Fan et
408 al., 2015), is also higher in *rb11* mutants than in wild types, and this effect is independent
409 of the environmental temperature (Suppl. Table 1 and Table 1). Besides TGD5, the
410 abundance of another TGD protein, namely TGD2, is also higher in *rb11* mutants when
411 exposed for 4 days to 4°C (Table 1). In addition, the chloroplast located protease systems
412 DegP2 and SPPA are also more abundant in cold treated *rb11* mutants when compared
413 to wild type (Table 1). Similarly, the inner envelope associated NADPH:protochloro-
414 phyllide reductase PORA (Barthélemy et al., 2000) appears, besides the TGD
415 components and FAX1, as a further RBL11 substrate (Suppl. Table 1), especially after
416 onset of cold temperature (Table 1). It seems likely that the decrease of some proteins in
417 *rb11* chloroplasts under warm or cold conditions represents pleiotropic reactions of the
418 mutant induced by altered FAX1 abundance (Suppl. Table 2 and Suppl. Table 3).
419 Nevertheless, among these proteins, we also found proteins associated with lipid
420 metabolism, e.g., LACS9, representing a major long chain acyl-CoA synthetase (Schnurr
421 et al., 2002), or BASS1, representing a sodium/pyruvate cotransporter (Furumoto et al.,
422 2011) (Suppl. Table 2 and Suppl. Table 3).

423

424 **FAX1 overexpressor lines exhibit markedly increased levels of FAX1 protein**

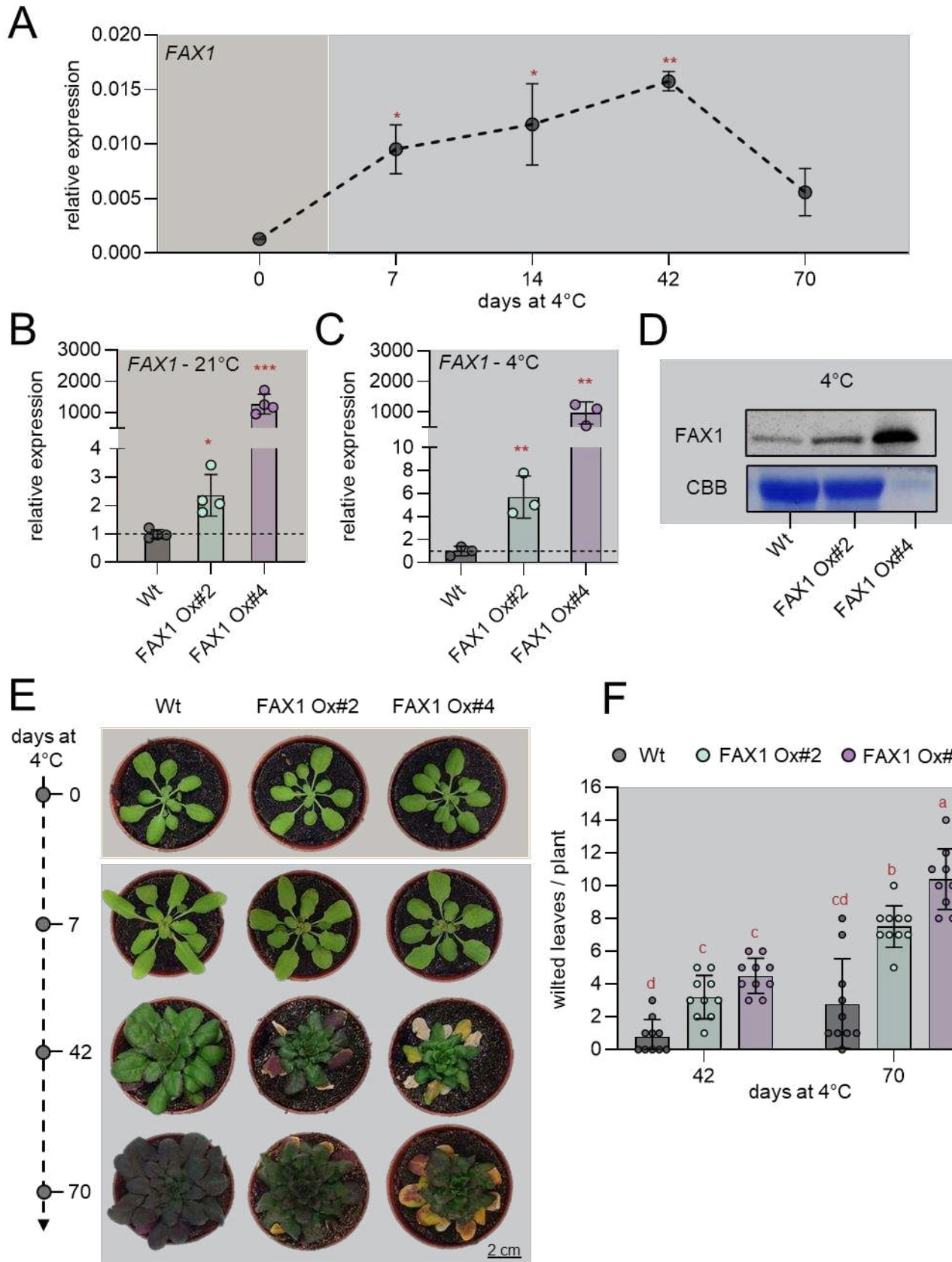
425 The above data indicate a molecular interrelation between increased FAX1 protein abundance
426 (due to an absence of RBL11) and the levels of membrane lipids and Arabidopsis
427 cold tolerance (Figures 1 and 3). This encouraged us to analyze the impact of increased
428 FAX1 abundance on plant cold tolerance. *rb/11* mutants are not conducive to this,
429 because the absence of this protease does not exclusively affect FAX1 levels, but also
430 the abundance of other envelope associated proteins (Table 1). To avoid the study of
431 pleiotropic effects, we decided to investigate the cold tolerance of Arabidopsis mutants
432 with constitutively increased FAX1 levels (Li et al., 2015).

433 Our observations that *rb/11* loss-of-function mutants have increased FAX1 levels under
434 cold conditions (Figure 1E) and that directed synthesis of RBL11 leads to a decrease in
435 FAX1 in the cold (Figure 2) provide evidence that the RBL11 protease is responsible for
436 this process. Nevertheless, for a comprehensive understanding of FAX1's impact on the
437 cold response, it is mandatory to study *FAX1* transcript levels after transfer to cold
438 conditions. In fact, the observation that *FAX1* mRNA rises markedly in wild-type plants
439 after exposure to 4°C (Figure 6A) supports our conclusion that RBL11 is responsible for
440 the cold-induced decrease of the level of the FAX1 protein (Figure 1F).

441 Previously, we generated two independent FAX1 overexpressing lines, FAX1 Ox#2 and
442 FAX1 Ox#4, both containing the *FAX1* gene under the control of the constitutive
443 cauliflower 35S promotor (Li et al., 2015). So far, it has only been shown that these mutant
444 lines have both, increased *FAX1* mRNA and increased FAX1 protein levels when grown
445 at ambient temperature (Li et al., 2015). We verified that the *FAX1* mRNA accumulation
446 is a stable feature when FAX1 overexpressor mutants are cultivated at cold temperature.
447 For this purpose, the *FAX1* mRNA levels were quantified in plants grown under the
448 standard temperature of 21°C with those grown for one week at 4°C. The two FAX1
449 overexpressor lines exhibited a substantial accumulation of *FAX1* mRNA when compared
450 to wild-type plants. Under warm temperature, FAX1 Ox#2 plants contained about 2.1-fold
451 higher *FAX1* mRNA levels as present in the wild type, while FAX1 Ox#4 plants contained
452 even 1170-fold higher *FAX1* mRNA (Figure 6B). This marked difference of *FAX1* mRNA
453 in the two overexpressors concurs with previous observations (Li et al., 2015). After one
454 week of growth at 4°C, FAX1 Ox#2 plants contained about 5.7-fold higher *FAX1* mRNA

455 levels, and FAX1 Ox#4 plants contained more than 970-fold higher *FAX1* mRNA levels
456 than present in the wild type (Figure 6C). Thus, even at 4°C, both FAX1 overexpressor
457 lines exhibited higher *FAX1* mRNA than present in the wild type.

458 It was shown that both FAX1 overexpressors contain higher levels of FAX1 protein when
459 grown at 21°C (Li et al., 2015). To confirm that also under cold conditions, FAX1
460 overexpressor lines exhibit higher FAX1 protein levels than present in wild types, we
461 conducted a immunoblot analysis (Li et al., 2015). After one week of growth at 4°C, the
462 relative FAX1 protein level in both overexpressor plants was higher than observed in wild
463 type plants (Figure 6D), and a corresponding quantification experiment revealed that
464 Ox#2 plants contained about 3-fold more FAX1 protein than present in wild type, while
465 Ox#4 plants contained about 115-fold more FAX1 protein (Figure 6D, please note: loaded
466 protein extracted from Ox#4 plants was 1:10 diluted when compared to proteins extracted
467 from wild types and Ox#2 mutants).



469 **Figure 6:** Gene expression, immunoblot and phenotypic analysis of two independent *Arabidopsis*
470 fatty acid export protein 1 (FAX1) overexpression lines (FAX1 Ox#2 and FAX1 Ox#4) and wild-
471 type (Wt) plants grown under standard and cold (4°C) conditions. Plants were grown under
472 standard conditions (21°C day and night, 10h day length and 120µE light intensity) for 3 weeks
473 and then treated with cold (4°C day and night, 10h day length and 120µE light intensity). A)
474 Expression of FAX1 by qRT-PCR under standard growth conditions (0 days at 4°C) and several
475 days during cold treatment (7; 14; 42, and 70 days at 4°C). Data represent relative mean
476 expression levels of 3 biological replicates and are normalised to standard conditions (0 days at
477 4°C) using UBQ as an internal control. Relative expression of FAX1 by qRT-PCR under B)
478 standard growth conditions and C) 7 days after cold treatment. Data represent relative mean
479 expression levels and are normalised to the wild type using UBQ as an internal control. D)
480 Immunoblot analysis of FAX1 in crude extract from plants grown at 4°C for 7 days. The image of
481 the Coomassie stained gel (CBB) shows equal loading of protein samples from Wt and FAX1
482 Ox#2 with 30µg per lane. The amount of FAX1 Ox#4 protein is reduced to 3µg. E) Rosette
483 phenotype of representative Wt, FAX1 Ox#2 and FAX1 Ox#4 under standard growth conditions
484 (0 days at 4°C) and after cold treatment (7; 42, and 70 days at 4°C). F) Number of wilted leaves
485 per plant after 42 and 70 days of cold treatment. Error bars in A) represent \pm SEM. Error bars in
486 B), C) and F) are \pm SD. Statistical differences between wild-type and overexpressor lines in A), B)
487 and C) were analysed by Student's t-test: p-value \leq 0.05: *; p-value \leq 0.01: **; p-value \leq 0.001: ***.
488 Letters above error bars in F) indicate significant differences by two-way ANOVA followed by
489 Tukey's test (p<0.05; (Supplemental file 1)).
490

491
492 **Similar to *rbf11* mutants, FAX1 overexpressor plants exhibit decreased chilling and**
493 **frost tolerance**

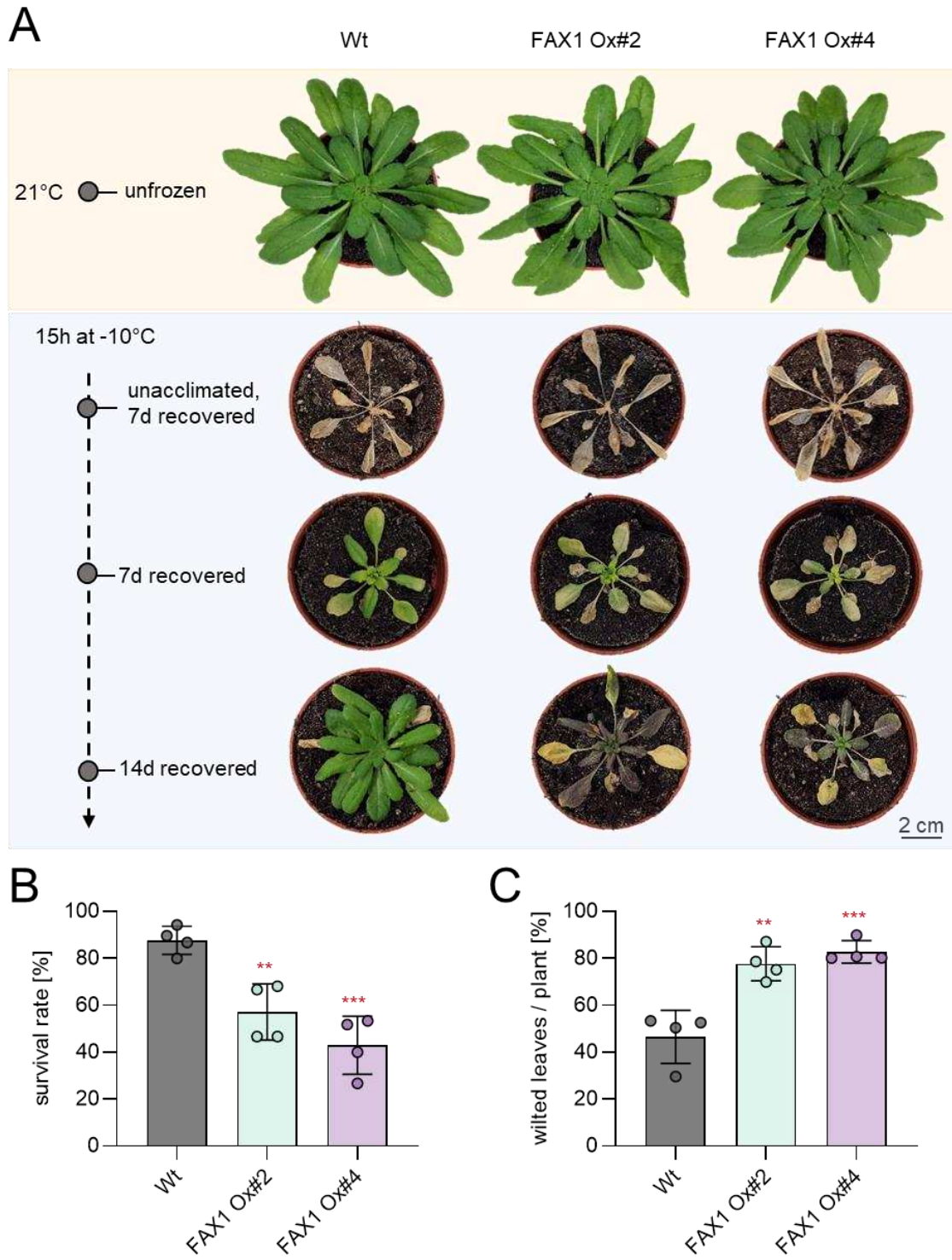
494 The data above indicate that *rbf11* mutants exhibit increased cold sensitivity (Figure 1B,
495 C). Because *rbf11* mutants revealed higher FAX1 levels than present in wild types it was
496 interesting to analyze whether the two lines constitutively expressing the *FAX1* gene also
497 show altered response to low temperatures.

498 Therefore, we cultivated all plants at ambient temperature (21°C) prior to cultivation at
499 4°C. Subsequently, we inspected morphologic plant appearance and the number of wilted
500 leaves in the respective growth phase. After 7 days at 4°C none of the three plant lines
501 developed wilted leaves (Figure 6E). However, after 42 days at 4°C, and even more
502 pronounced after 70 days at 4°C, leaves from both FAX1 overexpressors gradually wilted
503 more rapidly than observed in the wild type (Figure 6E).

504 To quantify this observation we counted the wilted leaves as a proxy for chilling sensitivity
505 (Trentmann et al., 2020). After 42 days at 4°C wild type plants exhibited on average one
506 wilted leaf while FAX1 overexpressor Ox#2 exhibited in average three wilted leaves, and

507 Ox#4 mutants showed in average 4.5 wilted leaves (Figure 6F). After growth for ten weeks
508 at 4°C, wild type plants displayed on average 2.8 wilted leaves per plant while FAX1
509 overexpressors Ox#2 and Ox#4 exhibited on average 7.5 and 10.4 wilted leaves,
510 respectively (Figure 6F).

511 As done for *rbf11* plants (Figure 2), we compared the frost tolerance of FAX1 over-
512 expressor plants and wild types. In contrast to both FAX1 overexpressors, wild types
513 which survived the post-freezing phase restored efficient growth within the next 14 days,
514 as indicated by a larger rosette size and less wilted leaves when compared to over-
515 expressor mutants (Figure 7A). FAX1 overexpressor plants able to recover from freezing
516 exhibited about 80% of wilted leaves, while wild types only exhibited about 46% of wilted
517 leaves (Figure 7A, B). With about 87% the survival rate of wild types reached a value
518 similar to previous observations (Trentmann et al., 2020). In contrast, only 57% of the
519 FAX1 Ox#2 plants survived this stress, and only 43% of FAX1 Ox#4 plants recovered
520 from frost (Figure 7C).



521

522 **Figure 7:** Recovery from frost is impaired in FAX1 overexpression mutants. Plants were cultivated
523 for 3 weeks under standard growing conditions. Before freezing the temperature was lowered to
524 4°C for 4 days (day and night temperature) for cold acclimation. Lowering of the temperature for
525 freezing was done stepwise (2°C/ h) and in completely dark. -10°C was kept for 15 h before a
526 stepwise temperature raising to 21°C (2°C/h). A) representative Wt and FAX1 overexpression
527 plants recovered from -10°C freezing. Pictures were taken 7 and 14 days after freezing, from

528 unacclimated and unfrozen (control) plants. B) Comparison of survival rate between Wt and FAX1
529 overexpression mutants 7 days after -10°C treatment. Data represent the mean value from four
530 independent experiments with 11 to 15 plants per line and experiment. C) Quantification of wilted
531 leaves from Wt and FAX1 overexpressor plants recovered for 7 days from -10°C freezing under
532 standard growing conditions. Data represent the mean value of 4 independent experiments.
533 Statistical differences between wildtype and the overexpressor lines in B) and C) was analyzed
534 by Student's t-test: p-value ≤0.01: **; p-value ≤0.001: *** (Supplemental File 1).

535

536

537 **Similar to *rbf11* mutants, lipid biosynthesis in FAX1 overexpressors is shifted to the**
538 **eukaryotic biosynthesis pathway under low temperature**

539 Under cold conditions, *rbf11* mutants exhibited a shift towards ER-synthesized membrane
540 lipids when compared to their corresponding wild type (Figure 5). To check whether this
541 response is due to high FAX1 protein abundance, we analyzed the lipid composition in
542 FAX1 overexpressors. For a first overview of cold effects on membrane lipid homeostasis
543 in FAX1 overexpressor plants, we grew wild types and the representative FAX1 Ox#4 line
544 (Li et al., 2015) under either control conditions, or for two weeks at 4°C. Subsequently,
545 leaf lipids were extracted and quantified via mass-spectrometry.

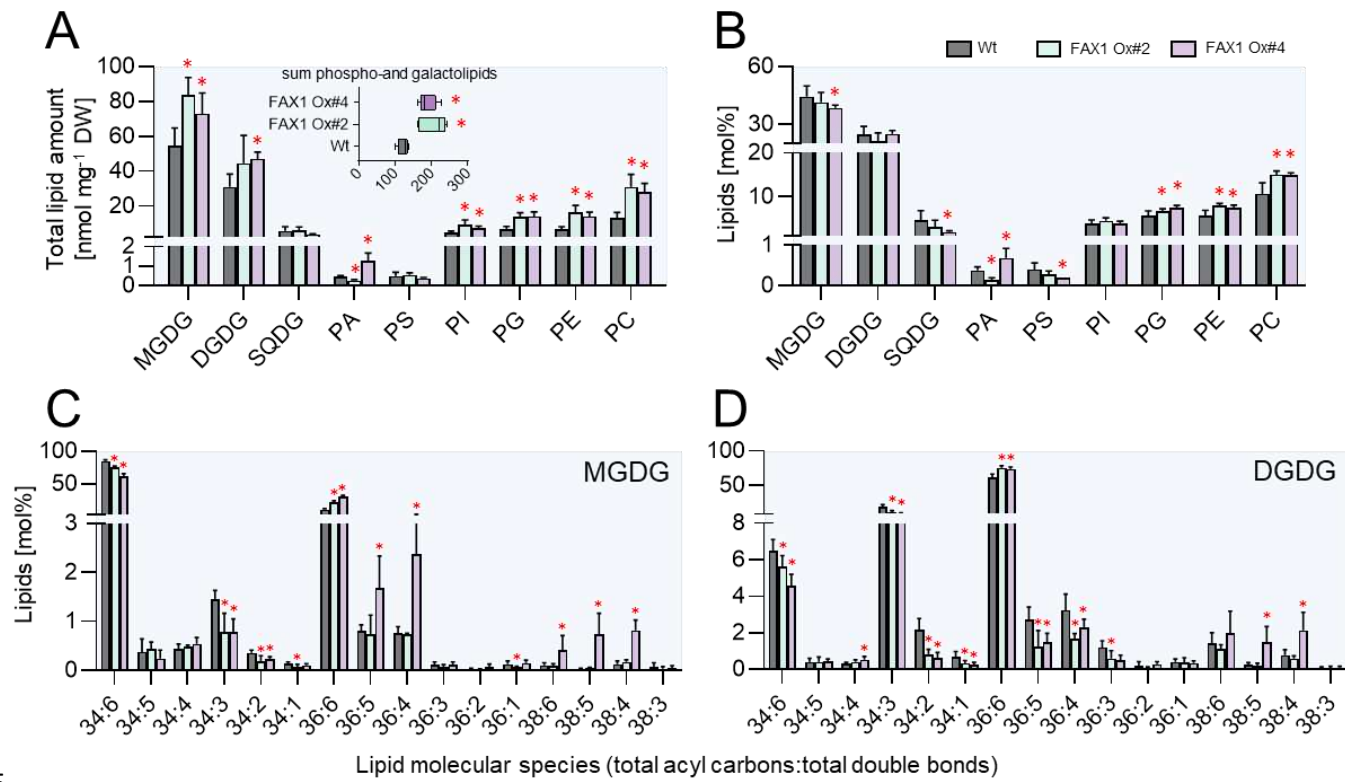
546 When grown at 21°C, the total levels (nmol mg⁻¹ DW) and the relative proportions (mol%)
547 of the glycolipids MGDG, DGDG and SQDG, or of the phospholipids PA, PS, PI, PG, PE
548 and PC were similar in leaves from wild types and FAX1 Ox#4 plants (Supplemental
549 Figure 1A, B and insert). In contrast, after two weeks at 4°C FAX1 overexpressor plants
550 contained higher levels of MGDG and DGDG when compared to wild types (Supplemental
551 Figure 1C). In addition, the levels of PS-, PG-, PE- and PC FAX1 Ox#4 plants appeared
552 to be slightly higher than in corresponding wild types (Supplemental Figure 1C). This
553 increase led in sum to 158 nmol mg⁻¹ DW of membrane lipids in FAX1 Ox#4 plants, while
554 wild types contained only 125 nmol mg⁻¹ DW membrane lipids (insert Supplemental Figure
555 1C). Similar to the situation at 21°C, the proportions of all lipid species in both plant lines
556 are nearly identical (Supplemental Figure 1D).

557 Since FAX1 overexpressor plants revealed impaired cold tolerance after long exposure to
558 low temperatures, and because the observed changes in lipid composition of FAX1
559 overexpressors after two weeks of growth at cold temperature appeared in parts to be
560 moderate (Supplemental Figure 1), we extracted lipids from plants exposed for ten weeks

561 to 4°C (Figure 8). Similar to plants exposed to only two weeks at 4°C (Supplemental Figure
562 1), both FAX1 overexpressor lines exhibited increased total levels of the galactolipids
563 MGDG and DGDG, and also of the phospholipids PI, PG, PE and PC (Figure 8A). The
564 increase of the two groups of lipids led to an overall higher level of total membrane lipids
565 in FAX1 overexpressor lines (FAX1 Ox#2, 205 nmol mg⁻¹ DW; FAX1 Ox#4, 188 nmol mg⁻¹
566 DW; wild type, 125 nmol mg⁻¹ DW; (insert Figure 8A). The levels of the low abundant
567 glycolipid SQDG and the phospholipid PS were not altered in FAX1 overexpressors, when
568 compared to wild type (Figure 8A). Although total amounts of glycolipids in both FAX1
569 overexpressors were higher when compared to wild types (Figure 8A), the relative
570 contribution (mol %) of MGDG, DGDG and SQDG in FAX1 Ox#2 and #4 to total
571 membrane lipids was similar to wild type (Figure 8B), while the relative contribution of the
572 phospholipids PG, PE and PC in FAX1 Ox#2 and #4 to total membrane lipids was
573 increased, when compared to the wild type (Figure 8B). The most pronounced alterations
574 of phospholipids were noted for PC and PE (Figure 8B), which were 40% higher in FAX1
575 overexpressors than in wild type plants (Figure 8B).

576 MGDG and DGDG represent the two most abundant glycerolipids in *Arabidopsis* leaves
577 (Figure 8A). Interestingly, a closer inspection of the contents of the two MGDG molecular
578 species 34:6 and 36:6 – which are indicative for either plastid-generated MGDG (34:6) or
579 ER-born MGDG (36:6) - revealed clear differences between wild types and
580 overexpressors. Wild-type plants exhibited about 85 mol% of 34:6 MGDG, while leaves
581 from FAX1 Ox#2 and Ox#4 plants accumulated only 75 and 62 mol% of this MGDG
582 species, respectively (Figure 8C). In marked contrast to this, wild type contained only 10
583 mol% of the MGDG molecular species 36:6, while the FAX1 overexpressor plants Ox#2
584 and Ox#4 accumulated 21 and 30 mol% of 36:6 MGDG, respectively (Figure 8C). The
585 relative levels of 34:6 and 34:3 DGDG in wild type leaves were higher than in
586 correspondingly grown FAX1 Ox#2 and Ox#4 plants. 34:6 DGDG in wild type amounted
587 at 6.5 mol%, while FAX1 Ox#2 and Ox#4 plants contained only 5.6 or 4.6 mol%,
588 respectively (Figure 8D). Eukaryotic ER-produced 36:6 DGDG in wild types amounted to
589 a relative abundance of 61 mol%, while, similar to the increase of 36:6 MGDG, the two
590 FAX1 overexpressors contained 75 and 74 mol% of 36:6 type DGDG, respectively (Figure
591 8D). In summary, we can conclude that FAX1 overexpressor lines at cold temperatures
592 accumulate ER-produced phospholipids – namely PC and PE – as well as galactolipids

593 (MGDG, DGDG) with DAG backbones from the eukaryotic pathway, while the proportions
594 of prokaryotic 34:x galactolipids are reduced.



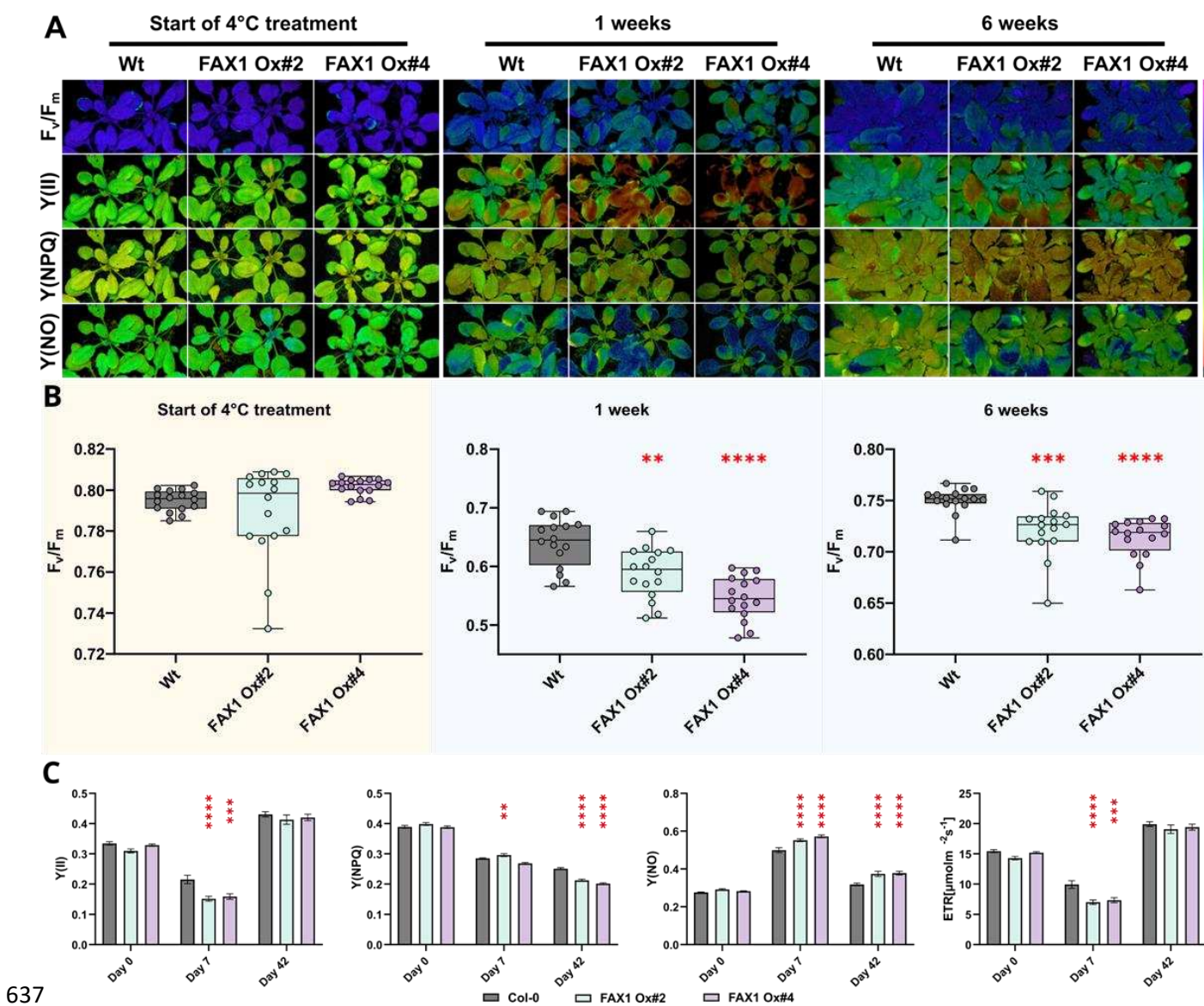
595
596 **Figure 8:** Lipid analysis of Wt and FAX1 overexpression lines. Galacto- and phospholipids as well
597 as galactolipid molecular species were determined in leaves of plants grown for 3 weeks under
598 standard conditions before lowering the growth temperature to 4°C for 10 weeks. Changes in A)
599 total contents and B) relative amounts of different galacto- and phospholipids. Boxplot in A)
600 indicates changes in the sum of measured total lipid contents. Lipid composition of C)
601 Monogalactosyldiacylglycerol (MGDG) and D) Digalactosyldiacylglycerol (DGDG) molecular
602 species. Data represent mean values of 5 plants per line. Error bars represent \pm SD. Significance
603 of differences between wildtype and mutant lines was analyzed by Student's t-test: p-value \leq 0.05: *
604 (Supplemental File 1).
605

606 **FAX1 overexpressor lines show symptoms of impaired photosynthesis at early time
607 points of cold exposure**

608 One marked phenotype of FAX1 overexpressor plants after transfer to cold conditions is
609 the appearance of wilted, decayed leaves after some weeks of growth (Figure 6F, H).
610 However, degradation of the FAX1 protein and first changes of the lipid composition are
611 already observed after a few days at 4°C (Figure 1F and Supplemental Figure 1). To
612 search for additional responses, we quantified photosynthetic parameters after short and

613 longer exposure to 4°C. To this end we grew all plants for 28 days at 21°C prior to transfer
614 to at 4°C. At the beginning of the transfer, and after one or six weeks of growth at 4°C, we
615 quantified the photosynthetic performance by measuring the following parameters: the
616 ratio of variable- to maximal fluorescence (F_v/F_m), PSII efficiency Y(II), non-photochemical
617 quenching Y(NPQ), non-regulated quenching Y(NO), and the rate of electron transport
618 (ETR). This comprehensive analyses have been done using the pulse-amplitude-
619 modulation (PAM) fluorometry method (Schreiber, 2004).

620 Prior to transfer to the cold, all wild type and the two FAX1 overexpressor plants exhibited
621 similar F_v/F_m ratios (Figure 9A) which ranged around 0.79 (Figure 9B). After onset of cold
622 temperatures, the F_v/F_m ratio decreased gradually in all three lines. Already after one
623 week, the F_v/F_m ratio in both FAX1 overexpressor lines was significantly lower than
624 displayed by the wild type, and after six weeks in the cold, wild type plants showed a F_v/F_m
625 ratio of 0.73, while both mutants exhibited a F_v/F_m ratio of about 0.68 (Figure 9A, B). This
626 altered F_v/F_m ratio in the cold is not reflected by an increased NPQ, although FAX1 Ox#2
627 plants showed a slightly increased NPQ, after 7 days in the cold. However, this was not
628 found for FAX1 Ox#4 plants (Figure 9) and even after 5 weeks in the cold, NPQ in all three
629 lines was similarly decreased (Figure 9C). The photosynthetic quantum yield Y(II) of all
630 three plant lines was similar when grown under control temperature (Figure 9C). In
631 contrast, both FAX overexpressors showed after 7 or 42 days in the cold a decreased
632 Y(II) and an increased energy dissipation via non-regulated quenching Y(NO), which was
633 especially pronounced after 42 days (Figure 9C). While the chloroplastic electron
634 transport rate (ETR) of all three plant lines was similar at the beginning of the cold
635 treatment, the ETR in both FAX1 overexpressor plants was after 7 days at 4°C markedly
636 lower, when compared to corresponding wild type plants (Figure 9C).



637

638 **Figure 9:** Cold-dependent PSII alterations in FAX1 over expressor lines. After 28 days of growth
639 under short-day (10/14 hours; 110 PAR) conditions at RT, plants (Col-0; FAX1 Oex#2; FAX1
640 Oex#4) were shifted to a 4°C short-day (110 PAR) chamber. Pulse-Amplitude-Modulation (PAM)
641 induction curve measurements at 110 PAR were performed on day 0 as well as after 7 days and
642 42 days of the cold treatment. A) Representative PAM images are depicted for PSII capacity
643 (F_v/F_m), yield ($Y(II)$), the quantum yield of light-induced non-photochemical fluorescence
644 quenching ($Y(NPQ)$), and quantum yield of nonregulated energy dissipation ($Y(NO)$). B) F_v/F_m
645 determination of the three genotypes at the start of the cold treatment, after one and five weeks.
646 C) Induction curves were generated until a steady-state phase of $Y(II)$, $Y(NPQ)$; $Y(NO)$, and
647 electron transport rate (ETR [$\mu\text{mol m}^{-2} \text{s}^{-1}$]) were reached. The data shown represents this steady-
648 state after 600 seconds. N = 16; Mean; \pm SEM; p-value: (one-way ANOVA): * = 0.033; ** = 0.0021;
649 *** = 0.0002; **** = 0.0001 (Supplemental File 1).

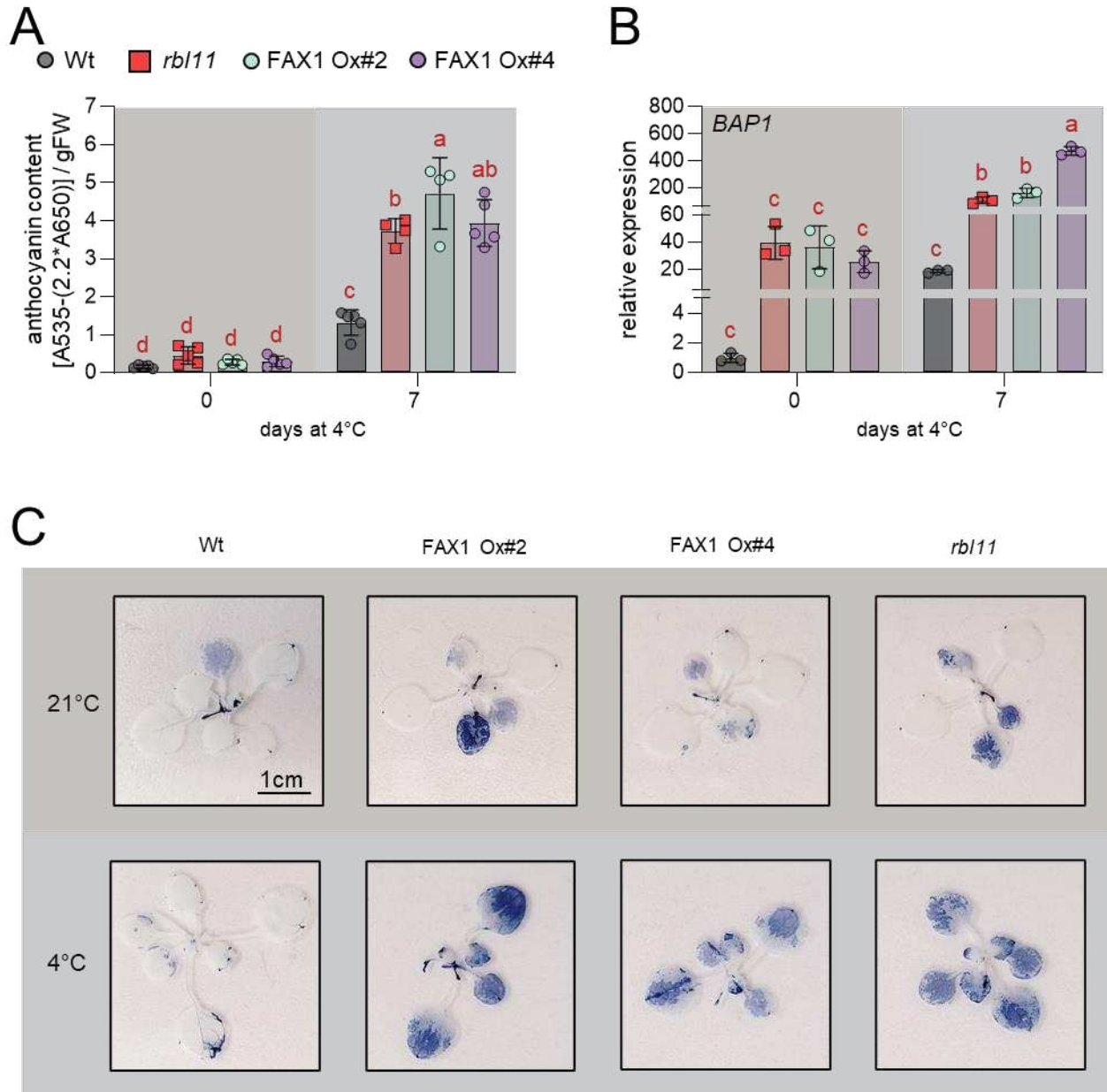
650

651 **FAX1 overexpressor and *rbf11* mutants exhibit signs of reactive oxygen species**
652 **(ROS) accumulation**

653 Several systemic changes in FAX1 overexpressors and *rbf11* mutants occur quite rapidly
654 after transfer to cold conditions. For example, first changes in the lipid composition of both
655 types of mutants are already present after two weeks at 4°C (Figure 5 and Supplemental
656 Figure 1) and alterations in photosynthetic parameters of FAX1 overexpressors are
657 already present after one week of growth at low temperature (Fig. 7). Given that both
658 types of mutants contain higher FAX1 abundance than present in wild types (Figures 1
659 and 4) and show similar shifts in lipid biosynthesis (Figure 5 and Supplemental Figure 1)
660 we searched for further similarities in their molecular responses after transfer into cold
661 conditions.

662 The accumulation of both, anthocyanins and reactive oxygen species (ROS) can be taken
663 as early responses upon onset of abiotic stress stimuli (Chalker-Scott, 1999; Baxter et al.,
664 2014). When grown at 21°C, *rbf11* plants and the two FAX1 overexpressor lines contain
665 similar levels of anthocyanins as wild type plants (Figure 10A). In contrast, when exposed
666 to 4°C for only one week, *rbf11* mutants and FAX1 overexpressors accumulated
667 significantly more anthocyanins than the correspondingly grown wild types (Figure 10A).
668 The levels of the transcript coding for the protein BAP1, which indicates the cold-induced
669 occurrence of ROS (Yang et al., 2007; Zhu et al., 2011), was unchanged between the
670 plant lines when grown at 21°C (Figure 10B). Similar to the anthocyanin accumulation,
671 *BAP1* mRNA accumulated to much higher extents in both types of mutants after one week
672 of growth at 4°C, than in wild type plants (Figure 10B).

673 To corroborate the differences in cold-induced ROS levels in wild types and the two types
674 of mutants, we analyzed the relative increase in leaf superoxide by nitroblue-tetrazolium
675 (NBT) staining (Doke, 1983; Hoffmann et al., 2013). NBT staining of wild-type tissue at
676 the start of cold treatment and after four days at 4°C does not result in a detectable
677 increase in superoxide (Figure 10C). However, both types of mutants showed a stronger
678 NBT staining after four days at 4°C than at the beginning of cold treatment (Figure 10C).



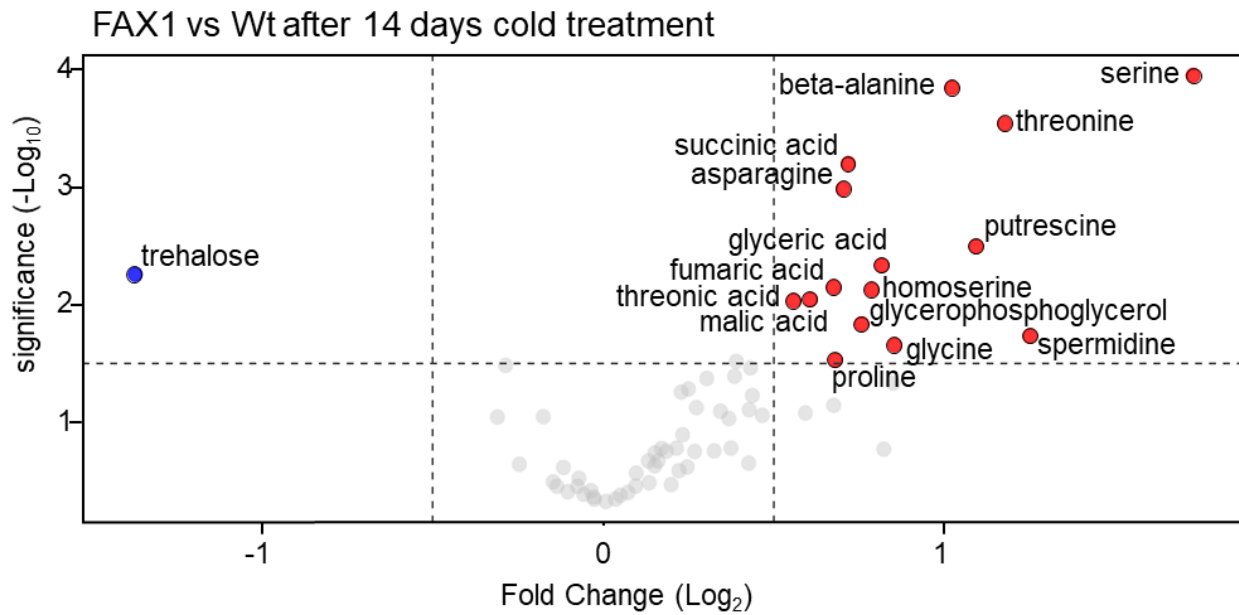
680 **Figure 10:** Anthocyanin and reactive oxygen species (ROS) accumulation in *rb11* loss of function
681 mutants and FAX1 overexpressors at low temperatures. A) Impact of cold on anthocyanin
682 accumulation under ambient conditions and after 7 days at 4°C. B) Relative transcript levels of
683 *BAP1* during standard conditions and after 7 days at 4°C. C) NBT staining of O₂⁻ accumulation.
684 Plants were grown for 2 weeks under control conditions and subsequently cultivated at 4°C for 4
685 days. Error bars in A) and B) represent ± SD. Letters displayed over the error bars indicate
686 significant differences analyzed by two-way ANOVA followed by Tukey's multiple comparisons
687 test (p-value <0.05; (Supplemental File 1)).
688

690 **FAX1 overexpressor plants exhibit altered levels of metabolites when exposed to**
691 **cold temperatures**

692 To gain additional insight into metabolic causes for the impaired cold- and frost tolerance
693 pattern of FAX1 overexpressor lines, we analyzed the levels of 71 primary metabolites via
694 GC-MS. Thus, wild-type plants and both FAX1 overexpressor lines were grown for 28
695 days at 21°C prior to growth at 4°C for two weeks.

696 When cultivated at 4°C for two weeks, the FAX1 overexpressor lines showed the largest
697 differences in their metabolic readjustment compared to correspondingly grown wild-type
698 plants (Figure 11, Supplemental Table 4). The two FAX1 overexpressor lines contained
699 nearly doubled levels of β -alanine, asparagine, serine and ethanolamine, 1.7-fold
700 increased amounts of glycerol-phosphoglycerol and 1.7-fold more malate when compared
701 to wild types (Figure 11). Similar to malate, three further intermediates of the tricarboxylic
702 acid cycle, namely citrate, fumarate and succinate were also significantly higher in cold
703 treated FAX1 overexpressors than in wild type plants (Figure 11). In addition, cold treated
704 FAX1 overexpressors contained about 38% more proline, about twice as much putrescine
705 and 2.3-fold more spermidine when compared to corresponding wild types, whereas the
706 trehalose concentration in FAX1 Ox#2 plants was substantially lower, compared to wild
707 types (Figure 11).

708



709
710 **Figure 11:** Volcano plot of the metabolic differences measured between Wt and FAX1 Ox#2
711 rosette leaves, cold treated for 14 days at 4°C. Blue dots represent decreased and red dots
712 increased metabolites with a \log_2 fold change ≥ 0.5 and $p\text{-value} \leq 0.05$. The complete data set is
713 available in Supplemental Table 4.
714 Significant differences between the 21°C and 4°C treatments were analyzed using a t-test
715 (Supplemental File 1).
716
717

718 **Discussion**

719 The dynamic modification of plant organelle proteomes is mandatory to achieve new
720 homeostatic levels allowing to cope with challenging environmental conditions (Taylor et
721 al., 2009). As seen in many systems, cellular mRNA level and the respective protein
722 amounts do not necessarily correlate to a high degree (Gygi et al., 1999; Greenbaum et
723 al., 2003; Koussounadis et al., 2015). Thus, other factors are also important for controlling
724 protein abundance. The chloroplast envelope proteome undergoes substantial remodel-
725 ing in response to changes in light or temperature conditions (Knopf et al., 2012;
726 Nishimura et al., 2016; Adam et al., 2019; Mielke et al., 2020) and it can thus be expected
727 that proteases must play a role for this.

728 Interestingly, cold-induced changes in the proteome are accompanied by modifications of
729 membrane lipids. Latter process maintains membrane fluidity at low temperatures and
730 stabilizes membrane integrity (preventing rigidification) to ensure proper organelle
731 function (Moellering et al., 2010; Zheng et al., 2011; Barnes et al., 2016; Barrero-Sicilia et
732 al., 2017; Guo et al., 2018). For lipid biosynthesis, especially for the generation of phos-
733 pholipids, fatty acid export from the chloroplast is mandatory. and the FAX1 protein is the
734 best characterized chloroplast envelope located protein presumed to be involved in this
735 transport process so far (Li et al., 2015; Li et al., 2016; Xiao et al., 2021).

736 In *Arabidopsis* FAX1 abundance rapidly decreases after transfer to cold temperatures
737 while other envelope proteins increase (Trentmann et al., 2020). Taking the proteins NTT
738 (the chloroplast ATP importer (Tjaden et al., 1998) or MEX1 (the chloroplast maltose
739 exporter) (Niittylä et al., 2004) as examples, we demonstrated that the relative changes
740 of these carriers are key to proper cold tolerance (Trentmann et al., 2020). However, in
741 the case of FAX1, it is unknown whether the decreased protein abundance is a controlled
742 process required to tolerate low environmental temperatures. In addition, no protease has
743 been discovered that could mechanistically explain the decreased abundance of selected
744 envelope-associated proteins in the cold.

745 Compared to *RBL10* and *FtsH11* mRNAs, the *RBL11* transcript accumulates early after
746 cold exposure (Figure 1A). This correlation is a first indication of a specific molecular
747 interaction between RBL11 and FAX1, and a physical contact between these two proteins,

748 which is a prerequisite for FAX1 degradation, was confirmed by BiFC analysis (Figure 2).
749 The suggestion of a specific effect of RBL11 on FAX1 abundance in the cold is supported
750 by two observations. First, cold-induced FAX1 degradation did not occur in *rb11* mutants
751 (Figure 1E), whereas *rb10* or *ftsh11* mutants degraded FAX1 in the cold similarly to wild-
752 type plants (Figure 1E). Second, dexamethasone-induced expression of RBL11 leads to
753 a decrease in FAX1 protein (Figure 4C).

754 In general, the ability of RBL11 to degrade intrinsic membrane proteins with multiple
755 transmembrane domains, such as FAX1 (Li et al., 2015), is consistent with the properties
756 of other rhomboid proteases (Erez and Bibi, 2009). However, since dexamethasone-
757 induced expression of RBL11 leads to FAX1 degradation only at cold temperature and
758 not at 21°C (Figure 4C), we propose a so far unknown post-translational modification of
759 RBL11 and/or FAX1, which is a prerequisite for catalytic protease activity (Figure 4C). The
760 observation that RBL11 activity might also be involved in the dynamic change TGD5 and
761 TGD2 (Table 1), two components of the TGD complex involved in the unidirectional ER
762 to plastids import of eukaryotic lipids (Xu et al., 2010; Li-Beisson et al., 2017), point to a
763 central function of this protease in modification of plant lipid homeostasis under
764 challenging temperature conditions. Notably, RBL10, the closest RBL11 homologue, has
765 also been shown to affect lipid metabolism as it interacts with the ACYL CARRIER
766 Protein4 and modulates MGDG biosynthesis (Lavell et al., 2019; Xu et al., 2023). Because
767 *rb11* mutants exhibit a shift toward eukaryotic lipid biosynthesis (which is due to
768 decreased FAX1 abundance but not observed in wild types, Figures 3 and 6,
769 Supplemental Figure 1), we hypothesize that *rb11* cells attempt to reduce the unintended
770 stimulation of eukaryotic lipid biosynthesis by downregulating the core plastid lipid
771 importer TGD (Table 1). This assumption is supported by the observation that Arabi-
772 dopsis, as a 16:3 plant, normally stimulates the plastid membrane lipid pathway after
773 exposure to cold conditions (Li et al., 2015; Yu et al., 2023).

774 Apart from FAX1 and TGD components, which act as substrates for RBL11, it is worth
775 mentioning that the protochlorophyllide oxidoreductase PORA strongly accumulates in
776 *rb11* mutants (Table 1). PORA is responsible for the stromal conversion of
777 protochlorophyllide to chlorophyllide and it was shown, that increased protochlorophyllide
778 oxidoreductase activity leads to ROS formation (Pattanayak and Tripathy, 2011). Thus,

779 RBL11 might not only contribute to the regulation of FAX1 activity but also influence
780 envelope-located mechanisms preventing cold-induced ROS formation.

781 *rb/11* mutants exhibit in cold conditions both, higher FAX1 protein levels than observed in
782 wild types (Figure 1E) and a shift of their lipid composition towards accumulation of
783 phospholipids (Figure 5). The latter observation is in accordance with both, the function
784 of FAX1 as a chloroplast to ER fatty acid (FA) export protein (Li et al., 2015; Li et al., 2016;
785 Li-Beisson et al., 2017; Takemura et al., 2019; Tian et al., 2019) and the function of the
786 ER as the cellular site of phospholipid biosynthesis (Li et al., 2015; Li et al., 2016; Li-
787 Beisson et al., 2017; Takemura et al., 2019; Tian et al., 2019). In fact, apart from a
788 stimulation of the eukaryotic pathway of lipid biosynthesis in the cold, *rb/11* plants and
789 FAX1 overexpressors share further similarities, e.g., impaired tolerance to low
790 temperatures and frost (Figures 1, 2 and 7), and increased levels of anthocyanins, ROS
791 and *BAP1* transcripts in the cold when compared to wild types (Figure 10A-C). Latter
792 changes are independent molecular markers for a reinforced stress situation in mutants
793 (Chalker-Scott, 1999; Choudhury et al., 2017)

794 Although in sum these similarities are indicative for an important function of the down
795 regulation of FAX1 during cold tolerance, a detailed analysis of the impact of FAX1 on this
796 process cannot be made in the *rb/11* mutants, since RBL11 acts on several inner envelope
797 proteins, which triggers pleiotropic effects in *rb/11* plants (Supplemental Tables 1 and 3,
798 and Table 1). Thus, the impact of FAX1 on cold and frost tolerance was analyzed using
799 FAX1 overexpressors. Although the relative abundances of *FAX1* mRNA and protein
800 differed substantially between Ox#2 and Ox#4 mutants, it turned out that the physiological
801 responses of the two plant lines were very similar (Li et al., 2015 and below). Accordingly,
802 these lines are suitable to search for a potential impact of a cold-induced down regulation
803 of FAX1 levels for tolerance to low temperatures.

804 The observation that FAX1 overexpressor leaves exhibited higher levels of ER-derived
805 membrane lipids (PE, PC) when exposed to cold temperature (Figure 8 and Supplemental
806 Figure 1B) indicates that the cold-induced decrease of FAX1 in wild types (Trentmann et
807 al., 2020) is a limiting factor for synthesis of lipid backbones via the eukaryotic pathway at
808 low temperature. Our assumption that a relative stimulation of lipid biosynthesis in the ER
809 is causative for increased total levels of galacto- and phospholipids in FAX1

810 overexpressors gains independent support by observations made on mutants lacking the
811 envelope proteins TGD2 or TGD3. Corresponding loss-of-function mutants show
812 decreased levels of MGDG and DGDG with ER-derived DAG-backbones, while ER-borne
813 phospholipid levels are increased (Awai et al., 2006; Lu et al., 2007). In other words, a
814 higher substrate availability such as acyl residues at the ER might lead to increased levels
815 of membrane lipids with ER-derived DAG backbones (Figure 12).

816 MGDG represents the most abundant chloroplast-located galactolipid (Dorne et al., 1990;
817 Kobayashi, 2016) and in the 16:3 plant *Arabidopsis*, two main molecular species occur
818 i.e., plastid derived 34:6 type MGDG and, as ER derived, 36:6 type MGDG (Boudière et
819 al., 2014). When compared to wild types, Ox#4 mutants grown at 21°C exhibit a relative
820 decrease of 34:6 type MGDG, which is nearly balanced by a corresponding increased
821 level of 36:6 type MGDG (Figure 8C), and the proportion of 34:6 DGDG is decreased,
822 while 36:6 DGDG is increased when comparing wild type with Ox#4 plants grown at 4°C
823 (Figure 8D). Thus, the latter observation indicates that a stimulated fatty acid export in
824 Ox#2 and Ox#4 plants leads to a shift from plastid-derived to ER-derived galactolipids.
825 Such flexible shift of lipid biosynthesis from plastids to the ER has already been observed
826 for mutants lacking the plastid glycerol-3-phosphate acyltransferase (ACT) activity
827 (Falcone et al., 2004; Lusk et al., 2022), and also in *act1* mutants (synonymous: *ats1*) a
828 stimulation of membrane lipid biosynthesis in the ER largely compensates for the impaired
829 prokaryotic lipid biosynthesis (Kunst et al., 1988). The observation that FAX1
830 overexpressors not only exhibit an increased ratio of 36:6 to 34:6 type MGDG (Figure 8C),
831 but also increased ratios of 36:6 to 34:6-, and 36:6 to 34:3 type DGDGs (Figure 8D) further
832 underlines the shift from prokaryotic to eukaryotic lipid biosynthesis in these lines. Finally,
833 the increase of the relative proportions of the two most abundant phospholipids, PC and
834 PE, supports the conclusion that the eukaryotic lipid biosynthesis pathway is stimulated
835 in FAX1 overexpressors.

836 The analyses of the molecular responses of the FAX1 mutants to cold and freezing
837 conditions showed that these changes are associated with a strongly impaired ability to
838 resist low environmental temperatures, as evidenced by an increased number of wilted
839 leaves in the cold and a decreased ability to recover from freezing (Figures 2 and 7). A
840 similar gradual decay of leaves was also seen for other *Arabidopsis* mutants exhibiting

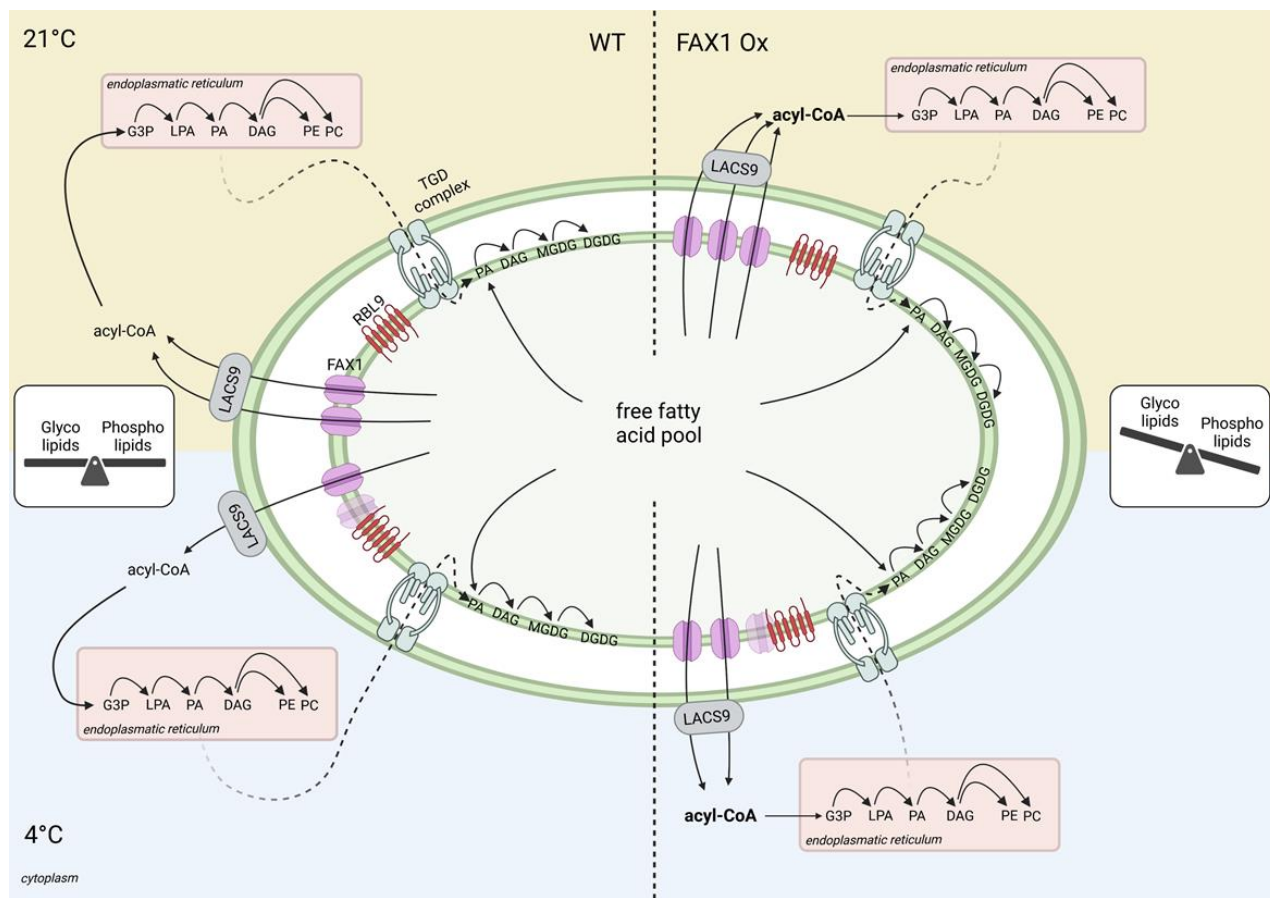
841 decreased amounts of polyunsaturated fatty acids in membrane lipids (Miquel et al., 1993)
842 and of course for the *rb/11* mutant (Figure 1). It seems likely, that the increased number
843 of wilted leaves of FAX1 overexpressors when grown at 4°C (Figure 6E and F) is the result
844 of an impaired photosynthetic performance (Figure 9A,C).

845 The exact reasons for these marked effects are not clear, but it was shown that changes
846 in the composition of membrane lipids, induced by modifications of different lipid
847 biosynthesis genes, affect photosynthetic properties (Botté et al., 2011; Kobayashi, 2016;
848 Gao et al., 2020). Thus, it seems conceivable that the altered chloroplast membrane
849 composition observed in FAX1 overexpressors (Supplemental Figure 1 and Figure 8) is
850 causative for the impaired photosynthetic performance. Indeed, the decreased F_v/F_m ratio
851 of FAX1 overexpressor plants (Figure 9A,B) is an indicator of impaired PSII function
852 (Murchie and Lawson, 2013) and a temperature stressed PSII can lead to ROS production
853 (Pospíšil, 2016), as observed in FAX1 overexpressor plants (Figure 10C-F). However, it
854 cannot be excluded that the marked effects of RBL11 mutation or FAX1 overexpression
855 on PC and PA levels (Figures 5C,D and 8A,B) also contribute to ROS accumulation
856 (Figure 10). This is because the signaling molecule PA has been shown to bind directly
857 to the plasma membrane NADPH oxidoreductase RBOHD, leading to the activation of this
858 enzyme. Accordingly, this process stimulates O_2^- production, which ultimately leads to
859 H_2O_2 accumulation (Zhang et al., 2009).

860 Wild-type plants and FAX1 overexpressor lines exhibit a quite similar metabolite pattern
861 when grown at 21°C. In contrast, the metabolite composition of FAX1 Ox plants during
862 growth at 4°C is to some degree indicative for reinforced cold stress. For example, the
863 comparably high accumulation of polyamines in form of putrescine and spermidine, of
864 amino acids like proline and asparagine, or the accumulation of the non-proteinogenic
865 amino acid β -alanine (Figure 11) represent independent evidences for a pronounced
866 metabolic response to cold temperatures (Alet et al., 2011; Liang et al., 2013; Zhang et
867 al., 2016; Marco et al., 2019; Parthasarathy et al., 2019). β -alanine is not only a metabolic
868 indicator for abiotic stress (Parthasarathy et al., 2019), it also acts as precursor for CoA
869 synthesis and is thus required for fatty acid and phospholipid biosynthesis (Perrett et al.,
870 2017). Therefore, β -alanine accumulation is coincident with higher total levels of galacto-
871 and phospholipids in FAX1 overexpressors in the cold (Figure 11A). Under many stress

872 conditions, asparagine and proline levels change similarly (Curtis et al., 2018). While the
873 exact function of asparagine during stress is unclear, the role of proline as a general stress
874 metabolite is well established (Liang et al., 2013; Ghosh et al., 2022). For example, proline
875 is able to diminish PS_{II} defects caused by rising ROS levels (Alia and Mohanty, 1997) and
876 because cold treated FAX1 overexpressors exhibit defects in PS_{II} activity (Figure 9A-C),
877 the induce proline accumulation might represent a process to tune down such negative
878 effects.

879 In summary, we propose a model in which the envelope protease RBL11 is responsible
880 for the degradation and down-regulation of FAX1 in cold-treated *Arabidopsis* plants
881 (Figure 12). This process represents a previously hidden molecular response that is
882 critical for optimal low temperature acclimation. Most likely, the initial cold response in
883 wild-type plants is represented by a preference for the prokaryotic lipid synthesis pathway
884 to protect chloroplast membranes and the photosynthetic machinery from cold damage.
885 Since the corresponding *FAX1* mRNA is not decreased in cold-treated wild-type plants
886 (Figure 6A), the decreased FAX1 protein level is most likely due to a specific effect of
887 RBL11. In near future it will be interesting to search for factors that activate RBL11 and/or
888 convert selected membrane proteins on the inner envelope proteins into specific
889 substrates (Figure 12). It seems worth to mention, that the cold-induced degradation of
890 FAX1 further supports findings on the importance of various chloroplast envelope
891 associated processes for plant cold and frost tolerance (Moellering et al., 2010; Barnes et
892 al., 2016; Guan et al., 2019; Schwenkert et al., 2023).



893

894 **Figure 12:** Proposed model for the influence of the fatty acid export protein1 (FAX1) abundance,
895 controlled by the envelope located rhomboid-like protease11 (RBL11), on cold adaptation via
896 balancing the glyco- and phospholipid contents in Arabidopsis.

897 In wild types, the the glyco- and phospholipid levels are balanced to gain ideal conditions for
898 growth and development under diverse environmental conditions. During low temperature, RBL11
899 interacts with FAX1, which leads to a decrease of FAX1 abundance. The associated reduced
900 export of fatty acids, and concomitted slowdown of the eukaryotic pathway for lipid biosynthesis,
901 seems to be an efficient mechanism for cold acclimation. In FAX1 overexpressing (Ox) plants
902 however, the permanent increased export of fatty acids from the chloroplast, which stimulates lipid
903 biosynthesis in the Endoplasmic Reticulum, leads to a shift to phospholipid synthesis. In FAX1 Ox
904 lines, RBL11 is unable to decrease FAX1 protein abundance, and the disturbed glyco- to
905 phospholipid ratio impairs the efficient acclimation to cold temperatures, results in cold- and frost
906 sensitive mutants.

907

908 **Material and Methods**

909 **Plant cultivation and growth conditions**

910 Arabidopsis (*Arabidopsis thaliana*) ecotype Columbia (Col-0) and transgenic plants were
911 sown on standard soil (type ED73, Einheitserde Patzer; Sinntal-Altengronau, Germany)
912 with 10% (v/v) sand, stratified at 4°C for 48 h and then grown under short-day regime (10
913 h light/14 h dark) at 60% relative humidity and 120 $\mu\text{mol m}^{-2} \text{s}^{-1}$ light intensity at 21°C,
914 representing standard growth conditions. For cold treatment, plants were grown for
915 21 days at 21°C first and subsequently transferred to a cultivation chamber (Fitotron
916 SGR223, Weis-Gallenkamp Technik, Heidelberg, Germany) and incubated for several
917 days at 4°C while all other parameters were kept constant.

918 We described FAX1 Ox#2 and FAX1 Ox#4 lines earlier (Li et al., 2015). *rbf10* mutants
919 (Lavell et al., 2019) were provided by Dr. Christoph Benning (Michigan State University,
920 Wisconsin, USA), *ftsh11* and *rbf11* mutants (Knopf et al., 2012; Adam et al., 2019) were
921 provided by Dr. Zach Adam (Hebrew University, Jerusalem, Israel).

922 For RNA extraction, metabolite and anthocyanin analysis, Arabidopsis rosette leaves
923 were collected five hours after onset of light, transferred immediately into liquid nitrogen
924 and stored at -80°C until preparation. Leaf material for chloroplast envelope isolation was
925 used directly after harvesting one hour before the start of illumination. For lipid isolation,
926 rosette leaves were collected and directly transferred in a glass tube containing boiling
927 water.

928

929 **Generation of RBL11 overexpressor lines**

930 The cloning steps to generate the dexamethasone-inducible RBL11 overexpression lines
931 were performed using S7 Fusion Polymerase™ (MD-S7-100, MobiDiag, Espoo, Finland).
932 The sequence of BirA-HA was first amplified from the Vector pcDNA3.1 MCS-
933 BirA(R118G)-HA (Roux et al., 2012) using gene-specific primers and ligated C-terminally
934 of *RBL11* in the pBSK vector (Short et al., 1988) by overlap extension PCR. The *RBL11*-
935 BirA-HA construct was amplified using gene-specific primers with *attB*-sites attached and

936 inserted first into pDONR and then into the destination vector pTA7001-DEST (Aoyama
937 and Chua, 1997) via the Gateway Cloning system.

938 Wildtype *Arabidopsis* plants were transformed via floral dip using *Agrobacterium*
939 *tumefaciens* (GV3101). Positive transformed plants were selected by hygromycin
940 selection (Harrison et al., 2006) and confirmed by Western Blot analysis using an HA-
941 antibody after induction of leaves with 30µM dexamethasone. Sequences of gene-specific
942 primers, which were used for cloning, are provided in Supplemental File 2

943

944 **Protein extraction from RBL11 overexpressor plants**

945 Prior to protein extraction, approximately 50 leaves of *Arabidopsis* wildtype, or RBL11-HA
946 overexpressor plants were cut and placed in 30µM DEX or water, as control. Leaves were
947 incubated on a shaker for 48h in a plant chamber at either 21°C, or 4°C. Preparation of
948 soluble and insoluble (membrane) protein fraction and detection of RBL11-HA using HA
949 antibody via Western Blot was performed as described earlier (Khan et al., 2018).

950

951 **Arabidopsis chloroplast envelope preparation**

952 *Arabidopsis* chloroplast envelope membranes were isolated according to an established
953 protocol (Bouchnak et al., 2018) with few modifications. In a cold room (4°C), before onset
954 of light, 100 to 200 g of rosette leaves were harvested from six-weeks old plants and
955 ground in a Waring blender (three cycles, each of 2 seconds, average intensity) in the
956 presence of grinding medium (Tricine-KOH (20 mM, pH 8.4), sorbitol (0.4 M), EDTA (10
957 mM, pH 8), and NaHCO₃ (10 mM), BSA (0.1% (w/v)). The homogenate was filtered
958 through one layer of Miracloth and centrifuged for 2 min at 2,070xg at 4°C. The
959 supernatant was discarded, and the sediment was gently resuspended on ice with a soft
960 natural bristle paint brush in washing medium (1x) (Tricine-KOH (10 mM, pH 7.6), sorbitol
961 (0.4 M), MgCl₂ (2.5 mM), and EDTA (1.25 mM)) with a final volume of the combined
962 chloroplast solutions = 24 ml). 6 ml of the suspension was equally distributed and loaded
963 on top of four continuous Percoll (Sigma Aldrich, Heidelberg, Germany) gradients
964 (containing 50% Percoll / 0.4 M sorbitol, prepared by centrifugation at 38,700xg, for 55

965 min at 4 °C). Loaded gradients were centrifuged for 10 min at 13,300xg, 4°C using a
966 swinging-bucket rotor. The intact chloroplasts present in the lower phase were retrieved
967 with a 10 ml pipet. The intact chloroplast suspension was washed twice with 30 ml
968 washing buffer (1x) and centrifuged for 2 min at 2,070xg at 4°C. After washing, the purified
969 chloroplasts were lysed by resuspending the sediment in hypotonic medium (MOPS (10
970 mM, pH 7.8), MgCl₂ (4 mM), PMSF (1 mM, dissolved in isopropanol), benzamidine
971 hydrochloride hydrate (1 mM), and ε-amino caproic acid (0.5 mM). 3 ml of lysed
972 chloroplasts were loaded on top of two prepared sucrose gradients (4 ml of 0.93 M, 3 ml
973 of 0.6 M and 2.5 ml of 0.3 M sucrose). Gradients were ultracentrifuged for 1 h at 70,000xg,
974 4°C in a swinging-bucket rotor. The yellow band of both gradients (containing the
975 envelope fraction) was retrieved and pooled in one tube. The envelope suspension was
976 washed in 12 ml membrane washing buffer medium (MOPS (10 mM, pH 7.8), PMSF (1
977 mM), benzamidine hydrochloride hydrate (1 mM), ε-amino caproic acid (0.5 mM) and
978 ultracentrifuged again for 1 h at 110,000xg, 4 °C. Supernatants were aspirated by using
979 a water pump. Approximately 100 µl of membrane washing buffer was used to resuspend
980 the envelope sediment. Isolated envelopes were stored in liquid nitrogen until use.

981

982 **Bimolecular Fluorescence Complementation for interaction studies**

983 For the cloning of the BiFC constructs, the full-length sequences of *RBL11*, *FAX1* and
984 *FTSH11* were used. The coding sequences were amplified by PCR using S7 Fusion
985 Polymerase (MD-S7-100, Mobidiag, Espoo, Finland) and inserted first into pDONR and
986 then into the pUBC-cYFP and the pUBC-nYFP vectors via the Gateway cloning system
987 (Grefen et al., 2010). Half of a yellow fluorescent protein (nYFP or cYFP) is thus fused to
988 the C- terminus of *RBL11*, *FAX1*, or *FTSH11*. The resulting constructs were then
989 transformed into *Agrobacterium tumefaciens* strain GV3101. Transient expression in
990 tobacco (*N. benthamiana*) leaves of RBL11, FAX1, and FTSH11, each fused to an nYFP
991 or cYFP, was performed as described (Walter et al., 2004). *Nicotiana benthamiana* leaves
992 were infiltrated through the lower epidermis. After 5 days, leaves were analyzed using a
993 Leica TCS SP5II fluorescence microscope (Leica Instruments, Wetzlar, Germany) (514
994 nm excitation and 525-582 nm detection of emission through an HCX PL APO 63 × 1.2 W
995 water immersion objective).

996 Sequences of gene-specific primers, which were used for cloning, are provided in
997 Supplemental File 2.

998

999 **Frost recovery experiment**

1000 For detection of the ability to recover from frost, a freezing tolerance test was performed
1001 according to an established approach (Trentmann et al., 2020; Cvetkovic et al., 2021).
1002 Survival rates and the numbers of wilted leaves were documented after 7 days of recovery
1003 under standard growth conditions.

1004

1005 **Pulse Amplitude Modulation (PAM) Fluorescence Measurements**

1006 Photosystem II parameters at constant light intensities were monitored using an imaging
1007 PAM M-Series IMAG-K7 and the ImagingWinGigE V2.56p (WALZ, Würzburg, Germany)
1008 software. Induction curve settings were on default with 110 PAR as light intensity, 40 s
1009 delay- and 20 s clock-time. Dark adaptation of plants lasted 10 minutes, followed by a 615
1010 s long measurement monitoring PSII capacity (F_v/F_m), PSII effective photochemical
1011 quantum yield (Y(II)), the quantum yield of light-induced non-photochemical fluorescence
1012 quenching (Y(NPQ)) and quantum yield of nonregulated energy dissipation (Y(NO))
1013 (Genty et al., 1989; Kramer et al., 2004). All plants analyzed (Col-0, FAX1 Ox#2 and FAX1
1014 Ox#4) were grown for 28 days under short-day conditions (10/14 h; 110 μ E) at RT before
1015 being shifted for the duration of 6 weeks to 4°C (10/14 h, 110 μ E). PAM measurements
1016 were carried out on the day of the shift to 4°C, after one or six weeks in the cold.

1017

1018 **Determination of anthocyanin content**

1019 For anthocyanin quantification 1 ml of extraction buffer composed of H₂O, propanol and
1020 HCl (81:18:1) was added to 100 mg of fine grounded rosette plant material and incubated
1021 for 3 min at 95°C, while shaking at 650 rpm and stored over night at RT in full darkness.
1022 After centrifugation for 15 min at 12.500 rpm at RT, the supernatant was used for
1023 photometric quantification at E₁=535 nm and at E₂=650 nm. The extinction was
1024 determined and corrected ($E_{corr}=[E_{535}-(2.2 \cdot E_{650})] / mg\ FW$).

1025

1026

1027 **Metabolomics**

1028 Metabolite profiling was performed according to established protocols (Roessner et al.,
1029 2001; Lisec et al., 2006; Erban et al., 2007). In brief, from four plants per genotype and
1030 growth condition, 50 mg fresh weight (Fw) of ground rosette material was mixed, in a 1.5
1031 ml reaction tube, with 180 μ l of cold (-20°C) methanol containing internal standards (10 μ l
1032 ribitol, 0.2 mg ml⁻¹ in water and 10 μ l ¹³C-sorbitol, 0.2 mg ml⁻¹ in water). After 15 min of
1033 incubation at 70°C, the extract was cooled down to room temperature and carefully mixed
1034 with 100 μ l of chloroform and 200 μ l of water. To force phase separation, a 15 min
1035 centrifugation step at full speed was performed. Fifty μ l of the upper (polar) phase was
1036 dried *in vacuo* and stored at -80°C. For derivatization, the pellet was resuspended in 10
1037 μ l of methoxyamin-hydrochloride (20 mg ml⁻¹ in pyridine) and incubated for 90 min at 40°C.
1038 After addition of 20 μ l of BSTFA (*N,O*-bis[trimethylsilyl]trifluoroacetamide) containing 2.5
1039 μ l retention time standard mixture of linear alkanes (n-decane, n-dodecane, n-
1040 pentadecane, n-nonadecane, n-docosane, n-octacosane, n-dotriacontane), the
1041 preparation was incubated at 40°C for further 45 min.

1042 One μ l of each sample was injected into a GC–TOF–MS system (Pegasus HT, Leco, St
1043 Joseph, USA). Samples were automatically processed by an autosampler system (Combi
1044 PAL, CTC Analytics AG, Zwingen, Switzerland). Helium acted as carrier gas at a constant
1045 flow rate of 1 ml min⁻¹. Gas chromatography was performed on an Agilent GC (7890A,
1046 Agilent, Santa Clara, CA, USA) using a 30 m VF-5ms column with 10 m EZ-Guard column.
1047 The temperature of the split/splitless injector was set to 250°C, as well as the transfer line
1048 and the ion source. The initial oven temperature (70°C) was linearly increased to a final
1049 temperature of 350 °C by a rate of 9°C/min. Metabolites were ionized and fractionated by
1050 an ion pulse of 70 eV. Mass spectra were recorded at 20 scans s⁻¹ with an *m/z* 50– 600
1051 scanning range. Chromatograms and mass spectra were evaluated using ChromaTOF
1052 4.72 and TagFinder 4.1 software (Luedemann et al., 2008).

1053

1054 **RNA Extraction, cDNA synthesis and qRT-PCR**

1055 RNA was extracted from 50 mg of frozen and fine ground rosette leaf material from four
1056 biological replicates per genotype and growth condition using the NucleoSpin RNA Plant
1057 Kit (Macherey-Nagel, Düren, Germany), according to the manufacturer's protocol. The

1058 synthesis of cDNA from RNA was performed with the qScript cDNA Synthesis Kit
1059 (Quantabio, Beverly, MA, USA). Primers used for gene expression analysis via qRT-PCR
1060 are listed in Supplemental File 2. *AtUBQ* was used as reference gene for normalization.
1061

1062 **Nitroblue tetrazolium (NBT) staining**

1063 For ROS staining, O_2^- was detected by nitroblue tetrazolium staining (Fryer et al., 2002)
1064 in whole rosettes of two weeks old *Arabidopsis* plants cultivated as described above. For
1065 cold treatments, plants were transferred to 4°C for four days, while control plants were
1066 kept under standard conditions.

1067

1068 **Measurement of galacto-, phospho- and sulfolipids**

1069 For the analysis of lipids, plants were cultivated as described above and transferred from
1070 standard conditions to 4°C for 2 weeks, 10 weeks, or used directly. From 5 plants per
1071 genotype 100 mg fresh weight of rosette leaf material was harvested and immediately
1072 placed into a glass tube containing boiling water to prevent degradation of phospholipids
1073 through phospholipase D activity. The lipid extraction was performed with
1074 chloroform/methanol after deactivation of lipase activities by boiling the tissue in water as
1075 described earlier (Gasulla et al., 2013). Lipids were measured by tandem mass
1076 spectrometry (Q-TOF 6530 Agilent Technologies) and quantified by MS/MS experiments
1077 with internal standards following the strategy developed earlier (Gasulla et al., 2013; Welti
1078 et al., 2002).

1079

1080 **Immunoblotting**

1081 Per lane, 8 µg of isolated chloroplast envelope protein or 30 µg of freshly prepared protein
1082 extract from *Arabidopsis* leaf material were separated via SDS-PAGE (12%). The proteins
1083 in the gel were transferred onto a nitrocellulose membrane by a semi-dry blotting system
1084 (TransBlot® Turbo™ Transfer System, BIO RAD, Göttingen, Germany). The membrane
1085 was blocked in phosphate-buffered saline plus 0.1% (v/v) Tween 20 (PBS-T) with 3% milk
1086 powder for 1 h at room temperature, and then washed three times in PBS-T for 10 min.
1087 The membrane was incubated with a polyclonal rabbit antibody raised against FAX1 (Li
1088 et al., 2015) over night at 4°C at 1:1000 dilution. After three times of washing with PBS-T
1089 for 10 min, the membrane was incubated with a horseradish peroxidase (HPR) conjugated

1090 anti-rabbit antibody (Promega, Walldorf, Germany) diluted 1:10.000 in PBS-T with 3% milk
1091 powder for 1 h. The immunoreaction was visualized by chemiluminescence using ECL
1092 Prime Western blotting reagent (GE Healthcare, Karlsruhe Germany) and a Fusion Solo
1093 S6 (Vilber-Lourmat, Eberhardzell, Germany).

1094

1095 **Peptide Mass spectrometry**

1096 Enriched envelope fractions were precipitated in 80% acetone, digested in solution using
1097 Lys-C and trypsin, and resulting peptides were desalted as previously described (Hammel
1098 et al., 2018). Peptide mass spectrometry was performed using a nanoUHPLC-IM-MS
1099 system (nanoElute coupled to timsTOF Pro2, Bruker Daltonics, Bremen, Germany).
1100 Samples were directly loaded on a 25 cm, 75 µm ID, 1.6 µm particle size, C18 column
1101 with integrated emitter (Odyssey/Aurora ionopticks, Melbourne, Australia) set to 50 °C,
1102 and peptides were separated under a flow rate of 0.3 µl/min using buffers A (water, 0.1%
1103 formic acid) and B (acetonitrile, 0.1% formic acid). The gradient employed ramped from
1104 2% B to 25% B within 67 min, then to 37% B within 10 min, followed by washing and
1105 equilibration steps. The MS was operated in positive mode, electrospray voltage was set
1106 to 1.4 kV and spectra were recorded from 100 – 1700 m/z. A total of 10 MS/MS PASEF
1107 ramps (1/K₀ 0.6 – 1.43 V*s/cm²) with 100 ms duration were acquired per cycle, and target
1108 intensity for MS/MS was set to 14500 whereafter the precursors were excluded from
1109 fragmentation for 0.4 min.

1110

1111 **Protein Identification and Quantification**

1112 Acquired data were searched against the Uniprot protein sequences for *Arabidopsis*
1113 *thaliana* (UP000006548) using the FragPipe v19.1 processing pipeline choosing the
1114 default LFQ-MBR workflow with minor modifications: peptide length was set to a minimum
1115 of 6 amino acids, missed cleavages to 3, normalization of intensities across runs was
1116 omitted. Mass spectrometry raw and processed data have been deposited at the
1117 ProteomeXChange Consortium via the PRIDE partner repository (Perez-Riverol et al.,
1118 2021) with the dataset identifier PXD041219.

1119

1120

1121 **Data normalization and missing value imputation**

1122 Prior to computation of protein-level statistics, replicate groups were normalized using the
1123 median-of-ratios method (Anders and Huber, 2010). Subsequently, we computed global
1124 variance estimates and local gene-wise mean estimates to impute missing data points as
1125 independent draws from normal distributions. When a replicate group did not contain any
1126 measurement, the normal distribution was centered at an intensity corresponding to the
1127 5% quantile of all intensities. Proteins were excluded from statistical analysis according to
1128 two filter criteria. First, proteins were considered ineligible for downstream analysis if there
1129 was no biological replicate group with at least one reading. Second, only proteins reported
1130 to be localized to the envelope membrane were considered, either by association with
1131 matching Gene Ontology terms retrieved from UniProt or by entry in the manually curated
1132 AT_CHLORO database (Ashburner et al., 2000; Bruley et al., 2012; Consortium, 2021).

1133

1134 **Statistical Analyses**

1135 Statistical analyses regarding the proteomic data were based on log2 transformed
1136 imputed values. According to the experimental design which consisted of two factors
1137 (genotype and treatment) at each of two levels (wild type/mutant and normal/cold),
1138 changes in protein abundance were evaluated using two-way analysis of variance,
1139 ANOVA (Fisher, 1925). To account for multiple hypothesis testing, we controlled the False
1140 Discovery Rate (FDR) by computing q-values based on the ANOVA p-values as
1141 previously described by Storey (Storey and Tibshirani, 2003; Storey et al., 2004). All
1142 calculations were carried out using the FSharp.Stats library for statistical computing (Venn
1143 et al., 2023). Changes were considered to be significant if a q-value of 0.05 was not
1144 exceeded.

1145 For statistical analysis of the numerical data GraphPad Prism 9 and Microsoft Office Excel
1146 were used. Significant differences between two groups were analyzed by two-tailed
1147 Student's *t*-test. The software Shiny application (<https://houssein-assaad.shinyapps.io/TwoWayANOVA/>) was used for letter-based representation of all
1148 pairwise comparisons using popular statistical tests in two-way ANOVA. Statistical data is
1149 provided in Supplemental File 1.

1151

1152 **Accession numbers**

1153 Sequence data from this article can be found in the ARAMEMNON GenBank data library
1154 (<http://aramemnon.uni-koeln.de/>). *FAX1* (*At3g57280*), *FTSH11* (*At5g53170*), *RBL10*
1155 (*At1g25290*), *RBL11* (*At5g25752*), *BAP1* (*At3g61190*).

1156

1157 **Acknowledgments**

1158 Work in the labs from ML, H-HK, AF MS, TM and HEN was supported by the Deutsche
1159 Forschungsgemeinschaft (DFG) within the SFB/Transregio (TRR) 175, The Green Hub.

1160

1161 **References**

- 1162
- 1163
- 1164 **Abdallah F, Salamini F, Leister D** (2000) A prediction of the size and evolutionary origin of the proteome
1165 of chloroplasts of *Arabidopsis*. *Trends Plant Sci.* **5**: 141-142
- 1166 **Adam Z, Aviv-Sharon E, Keren-Paz A, Naveh L, Rozenberg M, Savidor A, Chen J** (2019) The chloroplast
1167 envelope protease FTSH11 – interaction with CPN60 and identification of potential substrates.
1168 *Front. Plant Sci.* **10**
- 1169 **Alberdi M, Corcuera LJ** (1991) Cold-acclimation in plants. *Phytochem.* **30**: 3177-3184
- 1170 **Alet Al, Sanchez DH, Cuevas JC, Del Valle S, Altabella T, Tiburcio AF, Marco F, Ferrando A, Espasandín FD,
1171 González ME, Ruiz OA, Carrasco P** (2011) Putrescine accumulation in *Arabidopsis thaliana*
1172 transgenic lines enhances tolerance to dehydration and freezing stress. *Plant Sig. Behav.* **6**: 278-
1173 286
- 1174 **Alia PS, Mohanty P** (1997) Involvement of proline in protecting thylakoid membranes against free radical-
1175 induced photodamage. *J. Photochem. Photobiol.* **38**: 253-257
- 1176 **Anders S, Huber W** (2010) Differential expression analysis for sequence count data. *Genome Biol.* **11**: R106
- 1177 **Andersson MX, Dörmann P** (2009) Chloroplast membrane lipid biosynthesis and transport. *In* AS
1178 Sandelius, H Aronsson, eds, *The Chloroplast: Interactions with the Environment*. Springer, Berlin,
1179 Heidelberg, pp 125-158
- 1180 **Aoyama T, Chua NH** (1997) A glucocorticoid-mediated transcriptional induction system in transgenic
1181 plants. *Plant J.* **11**: 605-612
- 1182 **Ashburner M, Ball CA, Blake JA, Botstein D, Butler H, Cherry JM, Davis AP, Dolinski K, Dwight SS, Eppig
1183 JT, Harris MA, Hill DP, Issel-Tarver L, Kasarskis A, Lewis S, Matese JC, Richardson JE, Ringwald M,
1184 Rubin GM, Sherlock G** (2000) Gene Ontology: tool for the unification of biology. *Nature Genetics*
1185 **25**: 25-29
- 1186 **Awai K, Xu C, Tamot B, Benning C** (2006) A phosphatidic acid-binding protein of the chloroplast inner
1187 envelope membrane involved in lipid trafficking. *Proc. Natl. Acad. Sci.* **103**: 10817-10822
- 1188 **Balsara M, Goetze TA, Kovács-Bogdán E, Schürmann P, Wagner R, Buchanan BB, Soll J, Böltner B** (2009)
1189 Characterization of Tic110, a channel-forming protein at the inner envelope membrane of
1190 chloroplasts, unveils a response to Ca^{2+} and a stromal regulatory disulfide bridge. *J. Biol. Chem.*
1191 **284**: 2603-2616

- 1192 Barnes AC, Benning C, Roston RL (2016) Chloroplast membrane remodeling during freezing stress is
1193 accompanied by cytoplasmic acidification activating SENSITIVE TO FREEZING2 Plant Physiol. **171**:
1194 2140-2149
- 1195 Barrero-Sicilia C, Silvestre S, Haslam RP, Michaelson LV (2017) Lipid remodelling: unravelling the response
1196 to cold stress in *Arabidopsis* and its extremophile relative *Eutrema salsugineum*. Plant Sci. **263**:
1197 194-200
- 1198 Barthélémy X, Bouvier G, Radunz A, Docquier S, Schmid GH, Franck F (2000) Localization of NADPH-
1199 protochlorophyllide reductase in plastids of barley at different greening stages. Photosynth. Res.
1200 64: 63-76
- 1201 Baxter A, Mittler R, Suzuki N (2014) ROS as key players in plant stress signalling
1202 3. J Exp Bot **65**: 1229-1240
- 1203 Botté CY, Deligny M, Roccia A, Bonneau A-L, Saïdani N, Hardré H, Aci S, Yamaryo-Botté Y, Jouhet J,
1204 Dubots E, Loizeau K, Bastien O, Bréhélin L, Joyard J, Cintrat J-C, Falconet D, Block MA, Rousseau
1205 B, Lopez R, Maréchal E (2011) Chemical inhibitors of monogalactosyldiacylglycerol synthases in
1206 *Arabidopsis thaliana*. Nat. Chem. Biol. **7**: 834-842
- 1207 Bouchnak I, Moyet L, Salvi D, Kuntz M, Rolland N (2018) Preparation of chloroplast sub-compartments
1208 from *Arabidopsis* for the analysis of protein localization by immunoblotting or proteomics. J. Vis.
1209 Exp.
- 1210 Boudière L, Michaud M, Petroutsos D, Rébeillé F, Falconet D, Bastien O, Roy S, Finazzi G, Rolland N,
1211 Jouhet J, Block MA, Maréchal E (2014) Glycerolipids in photosynthesis: Composition, synthesis
1212 and trafficking. Biochim. Biophys. Acta **1837**: 470-480
- 1213 Bruley C, Dupierris V, Salvi D, Rolland N, Ferro M (2012) AT_CHLORO: a chloroplast protein database
1214 dedicated to sub-plastidial localization. Front. Plant Sci. **3**: 205-205
- 1215 Chalker-Scott L (1999) Environmental significance of anthocyanins in plant stress responses.
1216 Photochemistry and Photobiology **70**: 1-9
- 1217 Chen J, Burke JJ, Velten J, Xin Z (2006) FtsH11 protease plays a critical role in *Arabidopsis* thermotolerance.
1218 Plant J. **48**: 73-84
- 1219 Choudhury FK, Rivero RM, Blumwald E, Mittler R (2017) Reactive oxygen species, abiotic stress and stress
1220 combination. Plant J. **90**: 856-867
- 1221 Consortium GO (2021) The Gene Ontology resource: enriching a GOld mine. Nucleic Acids Res **49**: D325-
1222 d334
- 1223 Curtis TY, Bo V, Tucker A, Halford NG (2018) Construction of a network describing asparagine metabolism
1224 in plants and its application to the identification of genes affecting asparagine metabolism in
1225 wheat under drought and nutritional stress. Food, Energy Sec. **7**: e00126-e00126
- 1226 Cvetkovic J, Haferkamp I, Rode R, Keller I, Pommerrenig B, Trentmann O, Altensell J, Fischer-Stettler M,
1227 Eicke S, Zeeman SC, Neuhaus HE (2021) Ectopic maltase alleviates dwarf phenotype and improves
1228 plant frost tolerance of maltose transporter mutants. Plant Physiol. **186**: 315-329
- 1229 Doke N (1983) Generation of superoxide anion by potato tuber protoplasts during the hypersensitive
1230 response to hyphal wall components of *Phytophthora infestans* and specific inhibition of the
1231 reaction by suppressors of hypersensitivity. Physiol. Plant Pathol. **23**: 359-367
- 1232 Dorne AJ, Joyard J, Douce R (1990) Do thylakoids really contain phosphatidylcholine? Proc. Natl. Acad. Sci.
1233 USA **87**: 71-74
- 1234 Erban A, Schauer N, Fernie AR, Kopka J (2007) Nonsupervised construction and application of mass
1235 spectral and retention time index libraries from time-of-flight gas chromatography-mass
1236 spectrometry metabolite profiles. Methods Mol. Biol. **358**: 19-38
- 1237 Fan J, Zhai Z, Yan C, Xu C (2015) *Arabidopsis* TRIGALACTOSYLDIACYLGLYCEROL5 interacts with TGD1,
1238 TGD2, and TGD4 to facilitate lipid transfer from the Endoplasmic Reticulum to plastids. Plant Cell
1239 **27**: 2941-2955

- 1240 **Fisher RA** (1925) Statistical Methods for Research Workers. Oliver and Boyd, Edinburgh, Scotland
1241 **Fryer MJ, Oxborough K, Mullineaux PM, Baker NR** (2002) Imaging of photo-oxidative stress responses in
1242 leaves. *J. Exp. Bot.* **53**: 1249-1254
1243 **Furumoto T, Yamaguchi T, Ohshima-Ichie Y, Nakamura M, Tsuchida-Iwata Y, Shimamura M, Ohnishi J,**
1244 **Hata S, Gowik U, Westhoff P, Brautigam A, Weber AP, Izui K** (2011) A plastidial sodium-dependent
1245 pyruvate transporter. *Nature* **476**: 472-475
1246 **Gao J, Lunn D, Wallis JG, Browse J** (2020) Phosphatidylglycerol composition is central to chilling damage
1247 in the *Arabidopsis fab1* mutant. *Plant Physiol.*: pp.01219.02020
1248 **Garcia-Molina A, Kleine T, Schneider K, Mühlhaus T, Lehmann M, Leister D** (2020) Translational
1249 components contribute to acclimation responses to high light, heat and cold in *Arabidopsis*.
1250 *iScience* **23**: 101331
1251 **Gasulla F, vom Dorp K, Dombrink I, Zähringer U, Gisch N, Dörmann P, Bartels D** (2013) The role of lipid
1252 metabolism in the acquisition of desiccation tolerance in *Craterostigma plantagineum*: a
1253 comparative approach. *Plant J.* **75**: 726-741
1254 **Genty B, Briantais J-M, Baker NR** (1989) The relationship between the quantum yield of photosynthetic
1255 electron transport and quenching of chlorophyll fluorescence. *Biochim. Biophys. Acta* **990**: 87-92
1256 **Ghosh UK, Islam MN, Siddiqui MN, Cao X, Khan MAR** (2022) Proline, a multifaceted signalling molecule in
1257 plant responses to abiotic stress: understanding the physiological mechanisms. *Plant Biol.* **24**: 227-
1258 239
1259 **Greenbaum D, Colangelo C, Williams K, Gerstein M** (2003) Comparing protein abundance and mRNA
1260 expression levels on a genomic scale. *Genome Biol.* **4**: 117
1261 **Grefen C, Donald N, Hashimoto K, Kudla J, Schumacher K, Blatt MR** (2010) A ubiquitin-10 promoter-based
1262 vector set for fluorescent protein tagging facilitates temporal stability and native protein
1263 distribution in transient and stable expression studies. *Plant J.* **64**: 355-365
1264 **Guan L, Denkert N, Eisa A, Lehmann M, Sjuts I, Weiberg A, Soll J, Meinecke M, Schwenkert S** (2019) JASSY,
1265 a chloroplast outer membrane protein required for jasmonate biosynthesis. *Proc. Natl. Acad. Sci.*
1266 **116**: 10568-10575
1267 **Guo L, Yang H, Zhang X, Yang S** (2013) Lipid transfer protein 3 as a target of MYB96 mediates freezing and
1268 drought stress in *Arabidopsis*. *J. Exp. Bot.* **64**: 1755-1767
1269 **Guo X, Liu D, Chong K** (2018) Cold signaling in plants: Insights into mechanisms and regulation. *J. Integr.*
1270 *Plant Biol.* **60**: 745-756
1271 **Gygi SP, Rist B, Gerber SA, Turecek F, Gelb MH, Aebersold R** (1999) Quantitative analysis of complex
1272 protein mixtures using isotope-coded affinity tags. *Nat. Biotechnol.* **17**: 994-999
1273 **Hagio M, Sakurai I, Sato S, Kato T, Tabata S, Wada H** (2002) Phosphatidylglycerol is essential for the
1274 development of thylakoid membranes in *Arabidopsis thaliana*. *Plant, Cell Physiol.* **43**: 1456-1464
1275 **Hammel A, Zimmer D, Sommer F, Mühlhaus T, Schröda M** (2018) Absolute quantification of major
1276 photosynthetic protein complexes in *Chlamydomonas reinhardtii* using quantification
1277 concatamers (QconCATs). *Front. Plant Sci.* **9**
1278 **Harrison SJ, Mott EK, Parsley K, Aspinall S, Gray JC, Cottage A** (2006) A rapid and robust method of
1279 identifying transformed *Arabidopsis thaliana* seedlings following floral dip transformation. *Plant*
1280 *Methods* **2**: 19
1281 **Hoffmann C, Plocharski B, Haferkamp I, Leroch M, Ewald R, Bauwe H, Riemer J, Herrmann JM, Neuhaus**
1282 **HE** (2013) From endoplasmic reticulum to mitochondria: absence of the *Arabidopsis* ATP
1283 antiporter Endoplasmic Reticulum Adenylate Transporter1 perturbs photorespiration. *Plant Cell*
1284 **25**: 2647-2660
1285 **Hölzl G, Dörmann P** (2019) Chloroplast lipids and their biosynthesis. *Ann. Rev. Plant Biol.* **70**: 51-81
1286 **Kerppola TK** (2008) Bimolecular fluorescence complementation (BiFC) analysis as a probe of protein
1287 interactions in living cells. *Ann. Rev. Biophys.* **37**: 465-487

- 1288 **Khan M, Youn JY, Gingras AC, Subramaniam R, Desveaux D** (2018) In planta proximity dependent biotin
1289 identification (BioID). *Sci. Rep.* **8**: 9212
- 1290 **Khodakovskaya M, McAvoy R, Peters J, Wu H, Li Y** (2006) Enhanced cold tolerance in transgenic tobacco
1291 expressing a chloroplast ω -3 fatty acid desaturase gene under the control of a cold-inducible
1292 promoter. *Planta* **223**: 1090-1100
- 1293 **Knopf RR, Feder A, Mayer K, Lin A, Rozenberg M, Schaller A, Adam Z** (2012) Rhomboid proteins in the
1294 chloroplast envelope affect the level of allene oxide synthase in *Arabidopsis thaliana*. *Plant J.* **72**:
1295 559-571
- 1296 **Kobayashi K** (2016) Role of membrane glycerolipids in photosynthesis, thylakoid biogenesis and
1297 chloroplast development. *J. Plant Res.* **129**: 565-580
- 1298 **Koevoets IT, Venema JH, Elzenga JTM, Testerink C** (2016) Roots withstanding their environment:
1299 exploiting root system architecture responses to abiotic stress to improve crop tolerance. *Front. Plant Sci.* **7**
- 1300 **Koussounadis A, Langdon SP, Um IH, Harrison DJ, Smith VA** (2015) Relationship between differentially
1301 expressed mRNA and mRNA-protein correlations in a xenograft model system. *Scientific Rep.* **5**:
1302 10775
- 1303 **Kramer DM, Johnson G, Kiarats O, Edwards GE** (2004) New fluorescence parameters for the determination
1304 of QA redox state and excitation energy fluxes. *Photosynth. Res.* **79**: 209
- 1305 **Kunst L, Browse J, Somerville C** (1988) Altered regulation of lipid biosynthesis in a mutant of *Arabidopsis*
1306 deficient in chloroplast glycerol-3-phosphate acyltransferase activity. *Proc. Natl. Acad. Sci. USA* **85**:
1307 4143-4147
- 1308 **Lavell A, Froehlich JE, Baylis O, Rotondo AD, Benning C** (2019) A predicted plastid rhomboid protease
1309 affects phosphatidic acid metabolism in *Arabidopsis thaliana*. *Plant J.* **99**: 978-987
- 1310 **Lavell AA, Benning C** (2019) Cellular organization and regulation of plant glycerolipid metabolism. *Plant
1311 Cell Physiol.* **60**: 1176-1183
- 1312 **Li-Beisson Y, Neunzig J, Lee Y, Philipp K** (2017) Plant membrane-protein mediated intracellular traffic of
1313 fatty acids and acyl lipids. *Curr. Opin. Plant Biol.* **40**: 138-146
- 1314 **Li-Beisson Y, Shorrosh B, Beisson F, Andersson MX, Arondel V, Bates PD, Baud S, Bird D, Debono A,
1315 Durrett TP, Franke RB, Graham IA, Katayama K, Kelly AA, Larson T, Markham JE, Miquel M,
1316 Molina I, Nishida I, Rowland O, Samuels L, Schmid KM, Wada H, Welti R, Xu C, Zallot R, Ohlrogge
1317 J** (2010) Acyl-lipid metabolism. *The Arabidopsis Book* **8**: e0133-e0133
- 1318 **Li N, Gügel IL, Giavalisco P, Zeisler V, Schreiber L, Soll J, Philipp K** (2015) FAX1, a novel membrane protein
1319 mediating plastid fatty acid export. *PLoS Biol.* **13**: e1002053
- 1320 **Li N, Xu C, Li-Beisson Y, Philipp K** (2016) Fatty acid and lipid transport in plant cells. *Trends Plant Sci.* **21**:
1321 145-158
- 1322 **Li Q, Zheng Q, Shen W, Cram D, Fowler DB, Wei Y, Zou J** (2015) Understanding the biochemical basis of
1323 temperature-induced lipid pathway adjustments in plants. *Plant Cell* **27**: 86-103
- 1324 **Liang X, Zhang L, Natarajan SK, Becker DF** (2013) Proline mechanisms of stress survival. *Antioxidants &
1325 Redox Signaling* **19**: 998-1011
- 1326 **Lin Y-S, Medlyn BE, Ellsworth DS** (2012) Temperature responses of leaf net photosynthesis: the role of
1327 component processes. *Tree Physiology* **32**: 219-231
- 1328 **Lisec J, Schauer N, Kopka J, Willmitzer L, Fernie AR** (2006) Gas chromatography mass spectrometry-based
1329 metabolite profiling in plants. *Nature Prot.* **1**: 387-396
- 1330 **Lu B, Xu C, Awai K, Jones AD, Benning C** (2007) A small ATPase protein of *Arabidopsis*, TGD3, involved in
1331 chloroplast lipid import. *J. Biol. Chem.* **282**: 35945-35953
- 1332 **Luedemann A, Strassburg K, Erban A, Kopka J** (2008) TagFinder for the quantitative analysis of gas
1333 chromatography-mass spectrometry (GC-MS)-based metabolite profiling experiments. *Bioinformatics* **24**: 732-737
- 1334
- 1335

- 1336 **Mackey KR, Paytan A, Caldeira K, Grossman AR, Moran D, McIlvin M, Saito MA** (2013) Effect of
1337 temperature on photosynthesis and growth in marine *Synechococcus spp.* *Plant Physiol.* **163:** 815-
1338 829
- 1339 **Marco F, Busó E, Lafuente T, Carrasco P** (2019) Spermine confers stress resilience by modulating abscisic
1340 acid biosynthesis and stress responses in *Arabidopsis* plants. *Front. Plant Sci.* **10**
- 1341 **Mielke K, Wagner R, Mishra LS, Demir F, Perrar A, Huesgen PF, Funk C** (2020) FtsH12 abundance
1342 modulates chloroplast development in *Arabidopsis thaliana*. *J. Exp. Bot.*
- 1343 **Miquel M, James D, Jr., Dooner H, Browse J** (1993) *Arabidopsis* requires polyunsaturated lipids for low-
1344 temperature survival. *Proc. Natl. Acad. Sci. USA* **90:** 6208-6212
- 1345 **Moellering ER, Muthan B, Benning C** (2010) Freezing tolerance in plants requires lipid remodeling at the
1346 outer chloroplast membrane. *Science* **330:** 226-228
- 1347 **Murchie EH, Lawson T** (2013) Chlorophyll fluorescence analysis: a guide to good practice and
1348 understanding some new applications. *J. Exp. Bot.* **64:** 3983-3998
- 1349 **Nakamura Y** (2017) Plant phospholipid diversity: emerging functions in metabolism and protein-lipid
1350 interactions. *Trends Plant Sci.* **22:** 1027-1040
- 1351 **Niittylä T, Messerli G, Trevisan M, Chen J, Smith AM, Zeeman SC** (2004) A previously unknown maltose
1352 transporter essential for starch degradation in leaves. *Science* **303:** 87-89
- 1353 **Nishimura K, Kato Y, Sakamoto W** (2016) Chloroplast proteases: updates on proteolysis within and across
1354 suborganellar compartments. *Plant Physiol.* **171:** 2280-2293
- 1355 **Obata T, Fernie AR** (2012) The use of metabolomics to dissect plant responses to abiotic stresses. *Cell.*
1356 *Mol. Life Sci.* **69:** 3225-3243
- 1357 **Parthasarathy A, Savka MA, Hudson AO** (2019) The synthesis and role of β -alanine in plants. *Front. Plant*
1358 *Sci.* **10:** 921
- 1359 **Pattanayak GK, Tripathy BC** (2011) Overexpression of protochlorophyllide oxidoreductase C regulates
1360 oxidative stress in *Arabidopsis*. *PLoS ONE* **6:** e26532
- 1361 **Patzke K, Prananingrum P, Klemens PAW, Trentmann O, Martins Rodrigues C, Keller I, Fernie AR,**
1362 **Geigenberger P, Böltner B, Lehmann M, Schmitz-Esser S, Pommerenig B, Haferkamp I, Neuhaus**
1363 **HE** (2019) The plastidic sugar transporter pSuT influences flowering and affects cold responses.
1364 *Plant Physiol.* **179:** 569-587
- 1365 **Perez-Riverol Y, Bai J, Bandla C, García-Seisdedos D, Hewapathirana S, Kamatchinathan S, Kundu**
1366 **Deepti J, Prakash A, Frericks-Zipper A, Eisenacher M, Walzer M, Wang S, Brazma A, Vizcaíno**
1367 **Juan A** (2021) The PRIDE database resources in 2022: a hub for mass spectrometry-based
1368 proteomics evidences. *Nucleic Acids Res.* **50:** D543-D552
- 1369 **Perrett M, Gothard M, Ludwig A, Rouhier KA** (2017) Identifying a source of β -alanine and its broader
1370 implications in *Arabidopsis thaliana* by GC/MS. *FASEB J.* **31:** 626.621-626.621
- 1371 **Pommerenig B, Ludewig F, Cvetkovic J, Trentmann O, Klemens PAW, Neuhaus HE** (2018) In concert:
1372 orchestrated changes in carbohydrate homeostasis are critical for plant abiotic stress tolerance.
1373 *Plant, Cell Physiol.* **59:** 1290-1299
- 1374 **Pospíšil P** (2016) Production of reactive oxygen species by photosystem II as a response to light and
1375 temperature stress. *Front. Plant Sci.* **7:** 1950
- 1376 **Pottosin I, Shabala S** (2016) Transport across chloroplast membranes: optimizing photosynthesis for
1377 adverse environmental conditions. *Mol. Plant* **9:** 356-370
- 1378 **Rawsthorne S** (2002) Carbon flux and fatty acid synthesis in plants. *Prog. Lipid Res.* **41:** 182-196
- 1379 **Roessner U, Lüdemann A, Brust D, Fiehn O, Linke T, Willmitzer L, Fernie A** (2001) Metabolic profiling
1380 allows comprehensive phenotyping of genetically or environmentally modified plant systems.
1381 *Plant Cell* **13:** 11-29
- 1382 **Roughan PG, Slack CR** (1982) Cellular organization of glycerolipid metabolism. *Ann. Rev. Plant Physiol.* **33:**
1383 97-132

- 1384 **Roux KJ, Kim DI, Raida M, Burke B** (2012) A promiscuous biotin ligase fusion protein identifies proximal
1385 and interacting proteins in mammalian cells. *J.Cell Biol.* **196**: 801-810
- 1386 **Schnurr JA, Shockley JM, de Boer GJ, Browse JA** (2002) Fatty acid export from the chloroplast. Molecular
1387 characterization of a major plastidial acyl-coenzyme A synthetase from *Arabidopsis*. *Plant Physiol.*
1388 **129**: 1700-1709
- 1389 **Schreiber U** (2004) Pulse-Amplitude-Modulation (PAM) fluorometry and saturation pulse method: an
1390 overview. *In* GC Papageorgiou, Govindjee, eds, *Chlorophyll a Fluorescence: A Signature of*
1391 *Photosynthesis*. Springer Netherlands, Dordrecht, pp 279-319
- 1392 **Schwenkert S, Fernie AR, Geigenberger P, Leister D, Möhlmann T, Naranjo B, Neuhaus HE** (2022)
1393 Chloroplasts are key players to cope with light and temperature stress. *Trends Plant Sci.* **in press**
- 1394 **Schwenkert S, Lo WT, Szulc B, Yip CK, Pratt AI, Cusack SA, Brandt B, Leister D, Kunz HH** (2023) Probing
1395 the physiological role of the plastid outer-envelope membrane using the oemIR plasmid collection.
1396 *G3* (Bethesda)
- 1397 **Short JM, Fernandez JM, Sorge JA, Huse WD** (1988) Lambda ZAP: a bacteriophage lambda expression
1398 vector with in vivo excision properties. *Nucleic Acids Res.* **16**: 7583-7600
- 1399 **Smallwood M, Bowles DJ** (2002) Plants in a cold climate. *Philos. Trans. R Soc. Lond. B Biol. Sci.* **357**: 831-
1400 847
- 1401 **Song Y, Chen Q, Ci D, Shao X, Zhang D** (2014) Effects of high temperature on photosynthesis and related
1402 gene expression in poplar. *BMC Plant Biol.* **14**: 111
- 1403 **Steponkus PL, Garber MP, Myers SP, Lineberger RD** (1977) Effects of cold acclimation and freezing on
1404 structure and function of chloroplast thylakoids. *Cryobiology* **14**: 303-321
- 1405 **Storey JD, Taylor JE, Siegmund D** (2004) Strong control, conservative point estimation and simultaneous
1406 conservative consistency of false discovery rates: A unified approach. *J. Royal Stat. Soc.* **66**: 187-
1407 205
- 1408 **Storey JD, Tibshirani R** (2003) Statistical significance for genomewide studies. *Proc. Nat. Acad. Sci.* **100**:
1409 9440-9445
- 1410 **Takemura T, Imamura S, Tanaka K** (2019) Identification of a chloroplast fatty acid exporter protein,
1411 *CmFAX1*, and triacylglycerol accumulation by its overexpression in the unicellular red alga
1412 *Cyanidioschyzon merolae*. *Algal Res.* **38**: 101396
- 1413 **Taylor NL, Tan Y-F, Jacoby RP, Millar AH** (2009) Abiotic environmental stress induced changes in the
1414 *Arabidopsis thaliana* chloroplast, mitochondria and peroxisome proteomes. *J. Proteom.* **72**: 367-
1415 378
- 1416 **Tian Y, Lv X, Xie G, Wang L, Dai T, Qin X, Chen F, Xu Y** (2019) FAX2 mediates fatty acid export from plastids
1417 in developing *Arabidopsis* seeds. *Plant Cell Physiol.* **60**: 2231-2242
- 1418 **Tjaden J, Schwöppe C, Möhlmann T, Neuhaus HE** (1998) Expression of the plastidic ATP/ADP transporter
1419 gene in *Escherichia coli* leads to a functional adenine nucleotide transport system in the bacterial
1420 cytoplasmic membrane. *J.Biol.Chem.* **273**: 9630-9636
- 1421 **Trentmann O, Mühlhaus T, Zimmer D, Sommer F, Schroda M, Haferkamp I, Keller I, Pommerenig B,**
1422 **Neuhaus HE** (2020) Identification of chloroplast envelope proteins with critical importance for cold
1423 acclimation. *Plant Physiol.* **182**: 1239-1255
- 1424 **van Meer G, Voelker DR, Feigenson GW** (2008) Membrane lipids: where they are and how they behave.
1425 *Nat. Rev. Mol. Cell Biol.* **9**: 112-124
- 1426 **Venn B, Mühlhaus T, Schneider K, Weil L, Zimmer D** (2023) FSharpStats: Release 0.4.11. . Zenodo
- 1427 **Wagner R, Aigner H, Pruzinská A, Jänkänpää HJ, Jansson S, Funk C** (2011) Fitness analyses of *Arabidopsis*
1428 *thaliana* mutants depleted of FtsH metalloproteases and characterization of three FtsH6 deletion
1429 mutants exposed to high light stress, senescence and chilling. *New Phytol.* **191**: 449-458
- 1430 **Wagner R, von Sydow L, Aigner H, Netotea S, Brugiére S, Sjögren L, Ferro M, Clarke A, Funk C** (2016)
1431 Deletion of FtsH11 protease has impact on chloroplast structure and function in *Arabidopsis*
1432 *thaliana* when grown under continuous light. *Plant, Cell Environ.* **39**: 2530-2544

- 1433 **Walker B, Ariza LS, Kaines S, Badger MR, Cousins AB** (2013) Temperature response of in vivo Rubisco
1434 kinetics and mesophyll conductance in *Arabidopsis thaliana*: comparisons to *Nicotiana tabacum*.
1435 *Plant Cell Environ.* **36**: 2108-2119
- 1436 **Walter M, Chaban C, Schütze K, Batistic O, Weckermann K, Näke C, Blazevic D, Grefen C, Schumacher K,**
1437 **Oecking C, Harter K, Kudla J** (2004) Visualization of protein interactions in living plant cells using
1438 bimolecular fluorescence complementation. *Plant J.* **40**: 428-438
- 1439 **Wang P, Hsu C-C, Du Y, Zhu P, Zhao C, Fu X, Zhang C, Paez JS, Macho AP, Tao WA, Zhu J-K** (2020) Mapping
1440 proteome-wide targets of protein kinases in plant stress responses. *Proc. Natl. Acad. Sci.* **117**:
1441 3270-3280
- 1442 **Wang Z, Benning C** (2012) Chloroplast lipid synthesis and lipid trafficking through ER-plastid membrane
1443 contact sites. *Biochem. Soc. Trans.* **40**: 457-463
- 1444 **Welti R, Li W, Li M, Sang Y, Biesiada H, Zhou HE, Rajashekhar CB, Williams TD, Wang X** (2002) Profiling
1445 membrane lipids in plant stress responses. Role of phospholipase D alpha in freezing-induced lipid
1446 changes in *Arabidopsis*. *J. Biol. Chem.* **277**: 31994-32002
- 1447 **Witz S, Panwar P, Schober M, Deppe J, Pasha FA, Lemieux MJ, Möhlmann T** (2014) Structure-function
1448 relationship of a plant NCS1 member--homology modeling and mutagenesis identified residues
1449 critical for substrate specificity of PLUTO, a nucleobase transporter from *Arabidopsis*. *PLoS ONE* **9**:
1450 e91343
- 1451 **Xiao Z, Tang F, Zhang L, Li S, Wang S, Huo Q, Yang B, Zhang C, Wang D, Li Q, Wei L, Guo T, Qu C, Lu K,**
1452 **Zhang Y, Guo L, Li J, Li N** (2021) The *Brassica napus* fatty acid exporter FAX1-1 contributes to
1453 biological yield, seed oil content, and oil quality. *Biotechnol. Biofuels* **14**: 190
- 1454 **Xu C, Moellering ER, Muthan B, Fan J, Benning C** (2010) Lipid transport mediated by *Arabidopsis* TGD
1455 proteins is unidirectional from the endoplasmic reticulum to the plastid. *Plant Cell Physiol.* **51**:
1456 1019-1028
- 1457 **Xu Y, Kambhampati S, Morley SA, Cook R, Froehlich J, Allen DK, Benning C** (2023) *Arabidopsis* ACYL
1458 CARRIER PROTEIN4 and RHOMBOID LIKE10 act independently in chloroplast phosphatidate
1459 synthesis. *Plant Physiol.*
- 1460 **Yang H, Yang S, Li Y, Hua J** (2007) The *Arabidopsis* BAP1 and BAP2 genes are general inhibitors of
1461 programmed cell death. *Plant Physiol.* **145**: 135-146
- 1462 **Yu L, Shen W, Fan J, Sah SK, Mavraganis I, Wang L, Gao P, Gao J, Zheng Q, Meesapyodsuk D, Yang H, Li**
1463 **Q, Zou J, Xu C** (2023) A chloroplast diacylglycerol lipase modulates glycerolipid pathway balance
1464 in *Arabidopsis*. *Plant J.* **in press**
- 1465 **Zhang J, Yang D, Li M, Shi L** (2016) Metabolic profiles reveal changes in wild and cultivated soybean
1466 seedling leaves under salt stress. *PloS One* **11**: e0159622-e0159622
- 1467 **Zhang Y, Zhu H, Zhang Q, Li M, Yan M, Wang R, Wang L, Welti R, Zhang W, Wang X** (2009) Phospholipase
1468 D α 1 and phosphatidic acid regulate NADPH oxidase activity and production of reactive oxygen
1469 species in ABA-mediated stomatal closure in *Arabidopsis*. *Plant Cell* **21**: 2357-2377
- 1470 **Zheng G, Tian B, Zhang F, Tao F, Li W** (2011) Plant adaptation to frequent alterations between high and
1471 low temperatures: remodelling of membrane lipids and maintenance of unsaturation levels. *Plant,*
1472 *Cell Environ.* **34**: 1431-1442
- 1473 **Zhu L, He S, Liu Y, Shi J, Xu J** (2020) *Arabidopsis* FAX1 mediated fatty acid export is required for the
1474 transcriptional regulation of anther development and pollen wall formation. *Plant Mol. Biol.* **104**:
1475 187-201
- 1476 **Zhu Y, Yang H, Mang H-G, Hua J** (2011) Induction of *BAP1* by a moderate decrease in temperature is
1477 mediated by *ICE1* in *Arabidopsis*. *Plant Physiol.* **155**: 580-588
- 1478